SDU

1996

UNIVERSITY

Journal of Emerging Technologies and Computing (JETC)

Journal of Emerging Technologies and Computing (JETC)

is a peer-reviewed, open-access national and international scientific journal. Thematic areas: Computer Science, Infocommunication Technologies, and Mathematics with Applied Aspects

Publisher: SDU University

The journal is registered and licensed as an online publication and printed journal by the Ministry of Information and Social Development of the Republic of Kazakhstan.

Certificate (Online publication): No KZ01VPY00120097

Certificate (Printed journal): No KZ71VPY00120098

ISSN: 3105-6342 (online)

ISSN: 3105-6334 (print)

Frequency: four times a year (March, June, September, December)

Website: https://jetc.sdu.edu.kz

Editorial Board

Ministry of Science and Higher Education of the Republic of Kazakhstan

SDU University

Journal of Emerging Technologies and Computing (JETC)

Volume 3, Issue 3 • December 2025

Kaskelen, Kazakhstan — 2025

CONTENTS

SECTION I
Computer Science

This section focuses on current research directions and applied advancements
in Computer Science, particularly in the areas of artificial intelligence,
software engineering, and intelligent systems.

Article

Breaking Barriers with AI: The Evolution and Challenges of Automated Sign Language Recognition

Mamta Joshi [1], Pranjul Khankriyal [1], Yashvi Chandola* [1], and Vivek Uniyal [1]

[1]Department of Computer Science & Engineering, Institute of Technology Gopeshwar, Uttarakhand

DOI: 10.47344/9z9bqn04

Abstract

Communication remains a significant challenge for individuals with hearing impairments and speech-related disabilities, especially when others are not familiar with sign language. Developing technologies that facilitate seamless communication for these individuals is crucial to promote equality for disabled people and accessibility for all. Sign language recognition systems have emerged as a promising solution, typically implemented using a hardware or software-based approach. Hardware solutions, such as sensor-equipped gloves, often pose usability and cost barriers, making them less appealing for widespread adoption. In contrast, software-driven approaches using artificial intelligence (AI), deep learning (DL) and machine learning (ML) offer a more practical and scalable alternative. This paper provides a complete review of recent developments in AI-based sign language recognition systems, with a particular attention towards deep learning architectures such as Convolution Neural Networks (CNNs). The aim is to evaluate current methodologies, highlight their strengths and limitations, and identify potential directions for future research to improve communication technologies for hearing-impaired people.

Keywords: Sign Language Recognition, Machine Learning, Deep Learning, Assistive Technology, Communication Accessibility.

I. Introduction

"As per National Institute on Deafness and Other Communication Disorder (NIH) approx. 7.7% of United States children of the age ranging between 3-17 has had disorder of voice, speech, language or swallowing in past year. Among these children around 67.7% have speech problem Hoffman HJ et al. (2015) [16]." An automated system to bridge the communication gap between

Email: mamtajoshi26dec@gmail.com
Email: shivamkhankriyal515@gmail.com
*Corresponding author: yashvi.chandola@gmail.com
Email: yashvi.chandola@gmail.com ORCID: 0000-0003-0601-7092
Email: vivekuniyal12@gmail.com ORCID: 0009-0002-8487-6351

Received: June 11, 2025. Reviewed: November 23, 2025. Accepted: December 9, 2025.

hearing-impaired individuals and others holds great promise in the context of AI advancements. Joze et al. (2018) [27]. Some of the research work showed the important aspect of training the model with Spatiotemporal Convolution to process continuous frames in case of video analysis and sign language translation. Their proposed architecture includes R(2+1)D in which they are able to achieve admirable results comparatively to Sports1M, Kinetics, UCF101, and HMDB51 with accuracy of 73.3% which is by far best published result in Sports1M Tran et al, (2018) [1]. Mostly sign language detection is categorised into hardware-based approach and software-based approach. Also keeping in note, the fact that wearing the armband all the time to sign could be uncomfortable and having less amount of data for model training. So far, the authors have seen that majority of research work concludes towards improving the software models and the concern about the lack of dataset availability, which is essential in the accuracy of the trained model.

A. Variations in Sign Languages

As it is encountered till now there are around 138 to 300 distinct sign languages, which is the first language for beyond 72 million hearing impaired people all over world, as signs and gestures varies according to religions and countries Hoffman HJ et al. (2015) [16]. Most of the sign languages are very different from others, which makes model Training and testing Language dependent. Also, datasets for each language are different, and due to the differences between these languages there are limited resources to train the models for sign Language Translation, which always turns out to be a major concern because larger the dataset, the more accurate the trained model will be Joze et al. (2018) [27], Albanie et al. (2020) [28]. The Figure 1 shows the different sign language datasets. Some Sign Languages which are commonly used are ASL(American Sign Language used by around 2,50,000-5,00,000

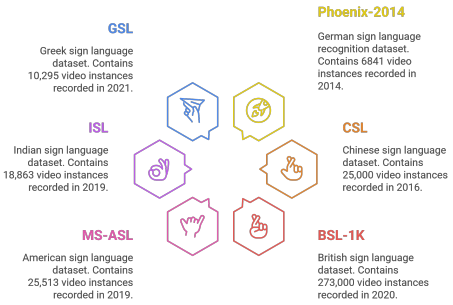

Fig. 1: Different Sign Language Datasets

people), BSL(British Sign Language used by 1,50,000 people), ISL(Indian Sign Language used by around 1 million to 2.7 million), CSL (Chinese Sign Language used by around 4.2 million peoples as per in 2021), DGS(German Sign Language used by 250,000 people) etc Li, Y., Zhang et al. (2022) [29]. According to Ethnologue and other sources (Joshi et al. [17], 2024; Sridhar et al., 2020 [26]), an estimated 1.5 million sign language users in India were reported to use Indo-Pakistani Sign Language (IPSL) as of 2008, making it one of the major sign languages in the region, shared with Pakistan and characterized by its own linguistic structure, though regional variations may exist; more recent studies suggest the number of users may have increased due to greater awareness and inclusion efforts, though precise updated figures remain limited, highlighting the need for further research and policy support to recognize and promote IPSL in education and accessibility initiatives

The Table I shows the different datasets available to facilitate the operation of training sign language translation models. Phoenix-2014 is a widely used benchmark for continuous sign language recognition. It includes weather forecast videos paired with German Sign Language (DGS) gloss annotations. It is often used to evaluate sequential modelling and translation pipelines. The Chinese Sign Language dataset contains continuous sequences with varied vocabulary and sentence structures. It supports research on region-specific sign recognition and gesture dynamics Li, Y., Zhang et al. (2022) [29]. One of the largest publicly available datasets for CSLR based on British Sign Language (BSL-1K). It includes a broad vocabulary, more than 1000 BSL Signs and many signers, making it suitable for developing signer-independent models Albanie et al. (2020) [28]. The MS-ASL dataset covers isolated sign recognition across 1,000 classes and more than 25,000 annotated videos of American Sign Language. It includes different signer in real-life recording condition enabling Machine Learning Models to understand ASL more Joze et al. (2018) [27]. The ISL is a dataset on Indian Sign Language created and used for the motive of training the machine learning model and research motives on

Received: June 11, 2025. Reviewed: November 23, 2025. Accepted: December 9, 2025.

TABLE I: Description of Sign Language Translation Datasets

Datasets	Language	Video Instances	Year	Type
Phoenix-2014 [2], [6]	German	6,841	2014	CSLR
CSL [2]	Chinese	25,000	2016	CSLR
BSL-1K [2], [6]	British	273,000	2020	CSLR
MS-ASL [4]–[6], [9]	American	25,513	2019	ISLR
ISL [10], [12], [13], [15]	Indian	18,863	2019	CSLR
GSL [4]	Greek	10,295	2021	CSLR

Note: CSLR: Continuous Sign Language Recognition, CSL: Chinese Sign Language dataset, BSL-1K: British Sign Language Dataset, MS-ASL: large-scale dataset in American Sign Language, ISL: Indian Sign Language Datasets, GSL: Greek Sign Language Datasets, ISLR: Isolated Sign Language Recognition.

Sign Language Translation Joshi et al. (2024) [17]. GSL is a large-scale dataset generated in Greek Sign Language which supports CSLR tasks. It is used for sign language recognition and translation Papadimitriou et al. (2024) [30]. In the Figure 2 the authors had categorised some of the widely used Sign Languages to show the differences between their very foundation. It can be observed in Figure 2(a) that ASL uses single hand to sign whereas in Figure 2(b) ISL and Figure 2(c) BSL uses both hands to sign. Also, almost every sign for alphabets in each language is different from others Albanie et al. (2020) [28].

B. Sign Language Translation

Sign Language Recognition for Models and Translation involves multiple stages to accurately identify sign gestures from the frame and translate these gestures into text or audio. Each step is very important on its own and plays an important role in maintaining the efficiency and accuracy of the translation system. Figure 3 shows the AI-Based sign language recognition system Cycle.

1) Data Collection and Preprocessing: In this process the raw video or image data of sign gestures is collected, they may vary in lighting or background noises to help in training the model in every possible criterion. Preprocessing involves operations like noise removal, background subtraction and gestures segmentation to prepare consistent inputs for the model and remove unnecessary overhead for the model Sridhar et al. (2020) [26]. The Figure 4 shows Steps for Preprocessing of collected data.

2) Feature Extraction and Selection: Appropriate features and gestures from the frame- including hand position, shape, orientation, facial expressions, and motion trajectories-are extracted. Classical methods like Histogram of oriented Gradients (HOG) and optical flow, while deep learning models extract features automatically using CNNs or 3D-CNNs Alzubaidi et al. (2021) [31], Al-Selwi et al. (2024) [32], Chen et al. (2021) [33].

3) Classification (Training and Testing): Extracted features are fed into classifiers (e.g., Random Forest, Neural networks or SVM) or end-to-end deep learning models. These systems are trained on labelled datasets and then tested to evaluate performance across various sign classes.

4) Sign-to-Text/Audio Translation: Recognized signs are mapped to their corresponding textual meaning. Using Natural Language Processing (NLP), grammatically correct sentences are generated and optionally converted to audio using text-to-speech (TTS) systems for real-time interaction Nadkarni et al. (2011) [20], Kumar et al. (2023) [21].

5) User Interface and Real-Time Application: A user-friendly interface enables deaf or hard-of-hearing individuals to interact with the system. Integration with cameras or mobile devices facilitates real-time translation in practical settings like classrooms, public services, or workplaces.

C. Challenges in AI- Based Sign Language Recognition

Many sign languages lack large, annotated datasets, especially for low-resource or regional languages. This scarcity limits the training capability of deep models and reduces generalizability Papadimitriou et al. (2024) [30]. Differences in hand size, speed, signing style, and facial expressions among users can reduce recognition accuracy. Models must be adaptable to signer-independent inputs. Unlike spoken languages, signs rely heavily on spatial grammar, body posture, and facial cues. Capturing and interpreting these nuances accurately requires multimodal fusion and temporal modelling Saunders et al. (2022) [24]. Deploying systems in real-world applications demands low latency and high frame-rate processing, which can be computationally intensive, especially on

Received: June 11, 2025. Reviewed: November 23, 2025. Accepted: December 9, 2025.

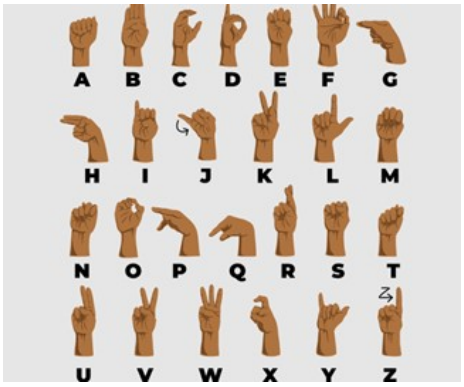

(a) American Sign Language (ASL)

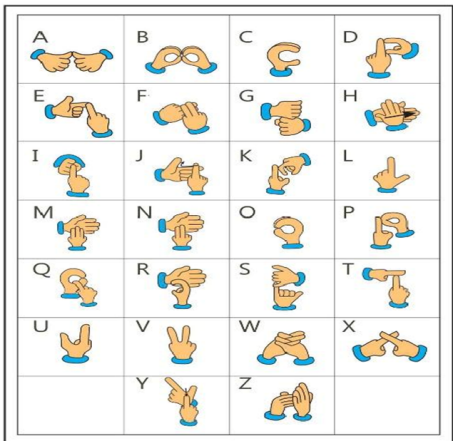

(b) Indian Sign Language (ISL)

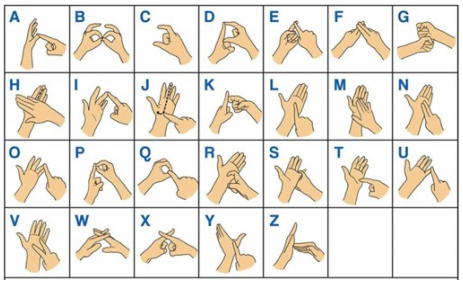

(c) British Sign Language (BSL)

Fig. 2: Comparison of sign language alphabets

edge devices or mobile platforms. Apart from these background clutters and uneven lighting can highly affect the efficiency of the model Kadam et al. (2020) [25]. The Figure 5 illustrates the Challenges in AI-Based Sign Language Recognition

II. Literature Review

Traditional methods for Sign language recognition (SLR) included sensor gloves which are hardware dependent, they are effective but has higher cost and may suffer the user from discomfort. Whereas with advancements in artificial intelligence (AI) and deep learning (DL), Sign Language Recognition has also evolved. Moreover, the focus of study has also shifted towards software-based approaches that utilize the concept of computer vision, neural networks and machine learning to interpret sign language. A major milestone in this domain is the introduction of spatiotemporal convolutional models, which drastically enhanced video-based action recognition. Tran et al. (2018) [1] proposed the R(2+1)D convolutional architecture in their paper, which is a model that separates spatial and temporal dimensions, demonstrating improved performance across several benchmark datasets like Sports1M and UCF101. This concept proves to be efficient for modelling dynamic hand gestures in continuous sign language recognition. Many thorough surveys have highlighted the fact of vast diversity among sign languages and the impact it has on dataset and sign language recognition system development. For instance, Madhiarasan and Roy (2022) [2] categorized sign languages by modality and regional variation, not taking accounts of the challenges for building a generalized models that can handle distinct grammar and gestures across ASL, BSL, ISL, and others. This leads to the requirement of the use of large, Sign language-specific datasets such as Phoenix-2014 for German Sign Language and MS-ASL for American Sign Language Joze et al. (2018) [27], Albanie

Received: June 11, 2025. Reviewed: November 23, 2025. Accepted: December 9, 2025.

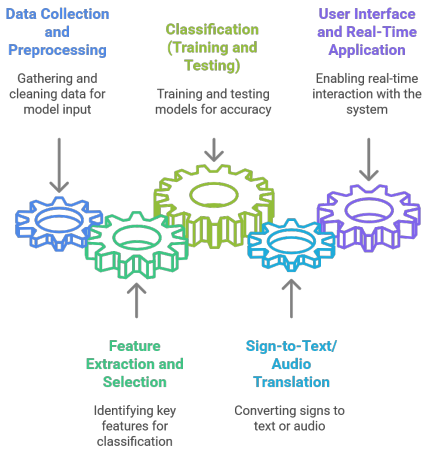

Fig. 3: AI-Based sign language recognition system Cycle

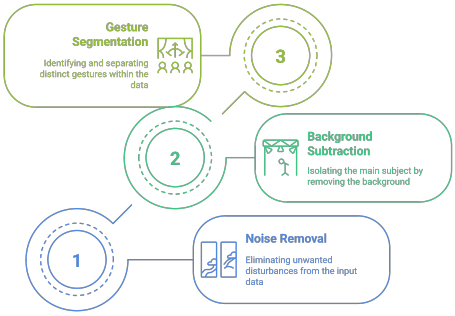

Fig. 4: Steps for Preprocessing of collected data

et al. (2020) [28], Li, Y., Zhang et al. (2022) [29]. To tackle the problem of processing complex multi-video input and user variability, Dignan et al. (2022) [3] developed a group-based recognition model that integrates multiple video streams to enhance classification accuracy. Their approach demonstrates that playing on diverse data perspectives can significantly affect the robustness of the system. Transformer-based models of Vaswani et al. (2017) [5] "Attention is All You Need," have also started to impact SLR architectures. The self-attention mechanism enables models to weigh temporal and spatial features more effectively and efficiently, which has proven useful in continuous sign translation Joze et al. (2018) [27]. Apart from architecture, Adeyanju et al. (2021) [6] critically evaluated machine learning approaches for SLR, identifying limitations in sign language recognition model such as overfitting, lack of performance in real-time, and difficulty in handling background clutter. They supported the use of hybrid models that integrates classical ML techniques with deep networks to reduce these concerns. A significant concern in the field is the scarcity of annotated datasets, especially for non-dominant languages. Subburaj and Murugavalli (2022) [12] noted that most public datasets are constrained in terms of signer variability, background complexity, and linguistic coverage. This data limitation hinders the development of truly scalable SLR systems Sridhar et al. (2020) [26]. Furthermore, several studies have underscored the importance of real-time processing and user adaptability. Najib (2025) [10] explored AI-driven models capable of real-time sign translation, incorporating speech synthesis and natural language processing (NLP) to fill the difference between gesture and spoken communication.

Received: June 11, 2025. Reviewed: November 23, 2025. Accepted: December 9, 2025.

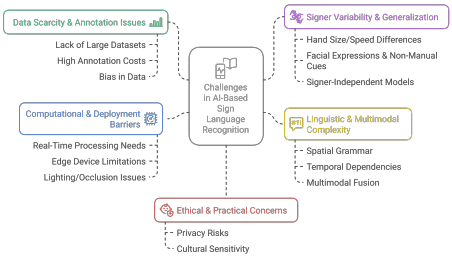

Fig. 5: Challenges in AI-Based Sign Language Recognition

The comparative Table II of SLR studies reveals several important patterns and trends that highlight the evolution of modelling strategies in the field. These results provide insights into researcher's decisions about input data, model settings, and application areas. Learning Rate controls how much the learning model will update its weight after each step. Batch size is defined as the number of samples processed before amending the model. Epoch means the model has seen all the training data once. Optimizer is termed as the algorithm that adjusts the weight. Dropout is a regularization technique to prevent overfitting as it randomly deactivates neurons during training. Learning rate schedule is a strategy in which the authors slowly increase at the beginning, it helps in stabilizing training in early stage of model training. the authors also observed that the demand for video-based input is growing, especially for the sign language recognition system models which are working on Continuous Sign Language Recognition (CSLR) Aloysius et al. (2020) [18]. Video-based methods have more hand movements, facial expression and temporal gestures in comparison to image-based methods. Work by Tran et al. (2018) [1] and Dignan et al. (2022) [3] provides that foundation for incorporating temporal features have greatly improved performance for dynamic signing Saunders et al. (2022) [24]. Most recent research has worked on deep learning models, particularly CNNs, RNNs, or CNN-LSTM combination models Al-Selwi et al. (2024) [32]. Typical hyperparameters are the batch sizes of 16–64, learning rates of approximately 0.001, and optimizers. These values were noticed to balance convergence speed with model stability, especially when the model is trained on medium-to-large datasets. Recent studies such as by Najib (2025) [10] and Papastratis et al. (2021) [4] indicate a growth in interest for the real time deployment of model for better usability and effectiveness. Lightweight models and inference speed are being top priority to consider, especially for mobile applications or assistive systems for deaf people and those who are hard-of-hearing.

A. Classical Machine Learning Techniques

The initial work in SLR were mostly based on hand-designed feature extraction and then machine learning classifiers. These methods needed manual design of features like hand orientation, trajectory, and position Adeyanju et al. (2021) [6], Oyeniran et al. (2020) [8].

- Support Vector Machines (SVMs) popularly used for gesture classification, SVMs showed high performance on limited datasets. They were particularly effective for isolated sign recognition tasks.
- Hidden Markov Models (HMMs) HMMs played a crucial role in modelling the temporal properties of gestures. They were able to capture sign transitions through time and were appropriate for sequential data such as CSLR.
- K-Nearest Neighbours (KNN) and Decision Trees were also used but often lacked scalability and robustness in complex, real-world settings.

While these models were computationally efficient, their dependence on manual features limited their generalizability across datasets and signers.

The Figure 6 shows Classical Machine Learning Techniques popularly used for sign language recognition.

The comparative Table III provides a summary about the studies that used classical machine learning methods in Sign Language Recognition system. It also stated the input type, task type, algorithms used for model and accuracy for these models. An accuracy of approximately 92 % has been achieved as highest among them.

B. Deep Learning-Based Approaches

With the rise of large datasets and computational power, deep learning transformed SLR by enabling automatic feature learning from raw image or video data Al-Qurishi et al. (2021) [22], Al-Selwi et al. (2024) [32]. The Figure 7 shows Deep Learning

Received: June 11, 2025. Reviewed: November 23, 2025. Accepted: December 9, 2025.

TABLE II: Studies carried out based on hyper parameters and input type for Sign Language Translation

Investigators (Year)	Input Type	Task Type	Key Hyperparameters	Description
Tran et al. (2014) [1]	Video	CSLR	Model's Learning Rate: 0.01, number of Epochs: 200, Batch Size: 16, Optimizer: SGD, Dropout: 0.5	R(2+1)D CNN, tested on Sports1M, UCF101
Dignan et al. (2022) [3]	Multi-Video	CSLR	Batch Size: 32, Epochs: 150, Optimizer: Adam	Fusion of multiple streams improves performance
Papastratis et al. (2021) [4]	Video	CSLR	Learning Rate of model: 0.001, number of Epochs: 100, Optimizer: Adam	LSTM + CNN hybrid for gesture sequence learning
Vaswani et al. (2017) [5]	Text (MLP base)	–	Learning Rate Schedule: Warm-up, Dropout: S0.1	Introduces Transformer, foundational in attention-based SLR models
Amrutha & Prabu (2021) [7]	Image	ISLR	Epochs: 100, Optimizer: Adam, Batch Size: 64	Simple CNN on Indian sign dataset
Bhaumik et al. (2023) [9]	Video	CSLR	Learning Rate: 0.0001, Batch Size: 32	Deep CNNs + NLP module for sentence translation
Najib (2025) [10]	Video	CSLR	Batch Size: 16, Optimizer: AdamW, Epochs: 120	End-to-end translation, Transformer backbone
Sultan et al. (2022) [11]	Image	ISLR	Dropout: 0.3, Batch Size: 64, Epochs: 80	Comparative study with CNN, MLP
Hussain et al. (2023) [15]	Video	CSLR	Batch Size: 32, Model's Learning Rate: 0.001	ISL-focused CNN-RNN architecture

Note: ISLR: Isolated Sign Language Recognition, LSTM: Long Short-Term Memory, CSLR: Continuous Sign Language Recognition, MLP: Multilayer Perceptron, RNN: Recurrent Neural Networks, SPORTS1M: Larger Dataset of YouTube videos, UCF101: Action Recognition Dataset, CNN: Convolution Neural Networks, BLEU: Bilingual Evaluation Understudy (for sign-to-text translation).

Techniques popularly used for sign language recognition.

1) Convolutional Neural Networks (CNNs): CNNs became foundational for image-based gesture recognition. By extracting hierarchical spatial features, CNNs significantly improved recognition accuracy Subburaj and Murugavalli (2022) [12], Amrutha and Prabu (2021) [7], Al-Qurishi et al. (2021) [22], Alzubaidi et al. (2021) [31], Al-Selwi et al. (2024) [32].

- Used effectively for static hand signs (e.g., alphabet recognition in ASL).
- Capable of learning complex spatial patterns like finger positions and hand shapes.
- Limitations include poor temporal understanding when used alone on video sequences.

2) Recurrent Neural Networks (RNNs) and LSTMs: To model temporal features in sign sequences, RNNs and their other variations like Long Short-Term Memory (LSTM) networks were introduced Papastratis et al. (2021) [4], Al-Selwi et al. (2024) [32].

- Effective for learning sequential relationships in continuous video.
- Can be integrated with CNNs (CNN-LSTM models) to learn spatial-temporal features.
- Suffer from limitations like vanishing gradients and high training time for long sequences.

3) 3D CNNs and Spatiotemporal Models: 3D CNNs can operates on spatial and temporal features concurrently Tran et al. (2018) [1], Alzubaidi et al. (2021) [31], Chen et al. (2021) [33]. Notable models include:

- C3D, I3D, and R(2+1)D: These extract features from frame sequences and learn motion dynamics.

Received: June 11, 2025. Reviewed: November 23, 2025. Accepted: December 9, 2025.

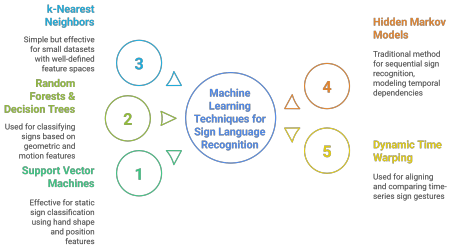

Fig. 6: Classical Machine Learning Techniques for SLR

TABLE III: Studies using Classical Machine Learning Approaches in Sign Language Recognition

Investigators	Input Type	Task Type	Algorithm Used	Accuracy
Adeyanju et al. (2021)	Image/Video	ISLR and CSLR	SVM, KNN, Decision Tree	80-92%
Amrutha and Prabu (2021) [7]	Image	ISLR	SVM	∼91%
Ozguizua et al. (2020)	Image/Video	ISLR	Naive Bayes, Decision Tree, KNN	78-88%
Nair and Bindu (2013)	Image	ISLR	Template Matching, HMM	∼80%
Sultan et al. (2022)	Image	ISLR	MLP, Decision Tree, KNN	85-89%
Hussain et al. (2023)	Image/Video	ISLR	SVM, Random Forest	∼90%

Note: Input type: static image frames or video sequences; Task type: ISLR (Isolated Sign Language Recognition) or CSLR (Continuous Sign Language Recognition).

- Particularly useful for CSLR, where the motion trajectory is vital.
- These models achieve higher accuracy but are computationally intensive.

The Table IV summarizes the studies that has improvised deep learning methods in Sign Language Recognition, it has also provided details about the input type, task type, model used and accuracy for these models. The maximum of 90 % accuracy has been reported approximately for the studies Al-Qurishi et al. (2021) [22].

4) Multimodal and Hybrid Models: Advanced systems often integrate multiple input types to improve robustness Dignan et al. (2022) [3]. Multimodal SLR combines vision (camera input), depth data (e.g., Kinect), and hand pose sensors. Hybrid Architectures use CNNs for feature extraction from image and LSTMs/Transformers for modelling of sequence. Some models integrate Natural Language Processing (NLP) for grammar-aware output and Text-to-Speech (TTS) systems for audio feedback. These approaches aim to replicate the richness of human communication by combining visual cues with linguistic and contextual processing.

The comparison Table V highlights the studies which uses multimodal or hybrid models in Sign Language Recognition, about their input type, task type, models used and their reported accuracy, an accuracy of 90 % approximately has been noted as highest for these models Sarhan et al. (2023) [19], Aloysius et al. (2020) [18].

5) Real-Time and Lightweight Models: Deploying SLR systems in real-world settings like mobile devices or AR glasses demands efficient models Najib (2025) [10], Papastratis et al. (2021) [4].

- Use of MobileNet, Tiny-YOLO, and quantized neural networks reduces computational cost Wang, W et al. (2020) [23].
- Techniques like frame skipping, model pruning, and knowledge distillation allow real-time inference without significant accuracy loss.

Received: June 11, 2025. Reviewed: November 23, 2025. Accepted: December 9, 2025.

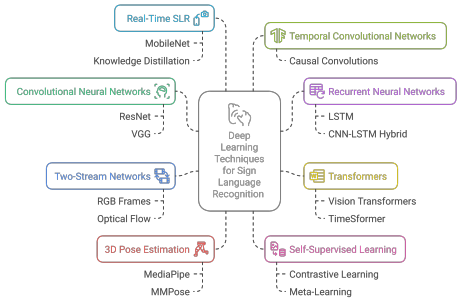

Fig. 7: Deep Learning Techniques for SLR

TABLE IV: Studies Using Deep Learning Techniques in Sign Language Recognition

Investigators	**Input Type**	**Task Type**	**Model Used**	**Accuracy**
Tran et al. (2018) [1]	Video	CSLR	R(2+1)D CNN	73.3% (Sports1M)
Dignan et al. (2022) [3]	Multi-Video	CSLR	Multi-stream CNN + Ensemble	∼85%
Papastratis et al. (2021) [4]	Video	CSLR	CNN + LSTM Hybrid	∼90%
Vaswani et al. (2017) [5]	Text (NLP)	–	Transformer	Foundational work
Bhaumik et al. (2023) [9]	Video	CSLR	Deep CNN + NLP	∼88%
Najib (2025) [10]	Video	CSLR	Transformer-based + TTS	∼89%
Ibrahim et al. (2020) [14]	Video	CSLR	Conceptual DL architectures	N/R
Subburaj and Murugavalli (2022) [12]	Video/Image	CSLR/ISLR	CNNs, RNNs (survey)	N/A

Note: Input type: video, multi-video streams or NLP inputs; Task type: ISLR (Isolated Sign Language Recognition) or CSLR (Continuous Sign Language Recognition); N/R: Not Reported; N/A: Not Applicable; TTS: Text-to-Speech.

Real-time models prioritize speed and energy efficiency, often at the expense of some precision, but are vital for practical adoption.

The Table VI provides the summary of studies which have used real-time and lightweight models in Sign Language Recognition illuminating the reported accuracy of the models used and their input type along with task types. A highest of 90% accuracy has reached approximately in the studies Sarhan et al. (2023) [19], Aloysius et al. (2020) [18].

The Table VII provides performance analysis of different Studies carried out in Sign Language Translation. The majority of high-performing models utilize video sequences as input, particularly for Continuous Sign Language Recognition (CSLR) Aloysius et al. (2020) [18], Sarhan et al. (2023) [19]. This trend reflects the importance of capturing motion dynamics and sequential dependencies in real-time signing, as seen in studies like those by Tran et al. (2018) [1] and Dignan et al. (2022) [3]. Static image inputs, used mainly in older or isolated sign models, tend to offer less contextual accuracy. Most studies prioritize accuracy as the primary metric, often accompanied by F1-score, precision, or recall. This dual focus ensures both correct classification and balance across varied sign classes. Some advanced systems, like Najib (2025) [10], also include BLEU scores for language-level evaluation, reflecting the evolution toward full sign-to-text translation pipelines. While only a few models (e.g., Najib (2025) [10], Hussain et al. (2023)

Received: June 11, 2025. Reviewed: November 23, 2025. Accepted: December 9, 2025.

TABLE V: Studies Using Multimodal or Hybrid Models in SLR

Investigators	Input Type	Task Type	Model + Algorithm	Accuracy
Dignan et al. (2022) [3]	Multi-Video Streams	CSLR	Multi-view CNN Ensemble	∼85%
Papastratis et al. (2021) [4]	Video + Sequential	CSLR	CNN + LSTM Hybrid	∼90%
Bhaumik et al. (2023) [9]	Video + NLP	CSLR	Deep CNN + Sentence NLP	∼88%
Najib (2025) [10]	Video + TTS	CSLR	Transformer + TTS	∼89%
Subburaj and Murugavalli (2022) [12]	Video/Image + Motion	CSLR/ISLR	Vision + Temporal Fusion	N/A

Note: ISLR: Isolated Sign Language Recognition, CSLR: Continuous Sign Language Recognition, CNN: Convolutional Neural Networks, LSTM: Long Short-Term Memory, TTS: Text-to-Speech, N/A: Not Applicable.

TABLE VI: Studies Using Real-time and Lightweight Models in SLR

Investigators	Input Type	Task Type	Model Used	Accuracy
Dignan et al. (2022) [3]	Multi-Video	CSLR	Multi-stream CNN (optimized)	∼85%
Papastratis et al. (2021) [4]	Video	CSLR	CNN + LSTM (low-latency)	∼90%
Najib (2025) [10]	Video + TTS	CSLR	Transformer (real-time)	∼89%
Hussain et al. (2023) [15]	Image/Video	ISLR	SVM + Fast Features	∼90%

Note: ISLR: Isolated Sign Language Recognition, CSLR: Continuous Sign Language Recognition, TTS: Text-to-Speech.

[15]) are explicitly designed for real-time processing, this capability is gaining importance. Real-time readiness is still constrained by computationally intensive demands, particularly with models using Transformers or 3D CNNs. Nevertheless, more recent studies increasingly focus on speed optimization in order to facilitate mobile and wearable deployment Wang, W et al. (2020) [23], Chen et al. (2021) [33].

III. Challenges and Limitations

Even though there are rapid advancement in deep learning and multimodal modelling systems, AI-based Sign Language Recognition system still faces significant challenges. These challenges include both the linguistic complexity (how complicated a particular sign language is?) and technical constraints of certain systems. The Figure 8 shows the major challenges and limitations in sign language recognition.

A. Dataset Scarcity and Lack of Standardization

One challenge that has been persistent in SLR research is the shortage of availability of large, different, and annotated datasets. Many datasets that are widely used such as MS-ASL, RWTH-PHOENIX, and BSL-1K are language-specific and often lack required signer diversity to train the learning model, real-world variability, or consistent annotation protocols for the accuracy and efficiency of model Madhiarasan and Roy (2022) [2], Subburaj and Murugavalli (2022) [12]. The lack of standardization in datasets makes it difficult to create a specific term for models to follow to generalize performance across languages Joze et al. (2018) [27], Albanie et al. (2020) [28], Li, Y., Zhang et al. (2022) [29], Papadimitriou et al. (2024) [30].

B. Co-Articulation and Temporal Segmentation

In continuous sign language recognition (CSLR), signs are not neatly segmented a s they are interconnected and gestures flow into one another, this is termed as a phenomenon known as co-articulation. Detecting the boundaries between individual signs

Received: June 11, 2025. Reviewed: November 23, 2025. Accepted: December 9, 2025.

TABLE VII: Performance of Studies for Sign Language Translation

Authors (Year)	Dataset Used	Metrics Reported	Real-Time	Signer Dependency
Tran et al. (2018) [1]	Sports1M, UCF101	Top-1:73.3%, Top-5	No	Dependent
Dignan et al. (2022) [3]	Custom (multi-video)	Acc:∼85%, Prec/Rec	Partial	Mixed
Papastratis et al. (2021) [4]	RWTH-PHOENIX	Acc, F1-score	Yes (Proto)	Independent
Vaswani et al. (2017) [5]	N/A	BLEU, Accuracy	Yes	N/A
Amrutha & Prabu (2021) [7]	Custom ISL	Acc:∼91%	No	Dependent
Bhaumik et al. (2023) [9]	MS-ASL	Acc:∼88%, TTS	Yes	Independent
Najib (2025) [10]	Custom Transformer	Acc, BLEU, Latency	Yes (Edge)	Independent
Sultan et al. (2022) [11]	ISL, MS-ASL	Acc, F1-score	No	Dependent
Nair & Bindu (2013) [13]	ISL	Acc:∼80%	No	Dependent
Hussain et al. (2023) [15]	ISL	Acc:∼90%, Speed	Yes	Mixed

Note: CSLR: Continuous SL Recognition, ISLR: Isolated SL Recognition, BLEU: Bilingual Evaluation Understudy, MS-ASL: American SL Dataset, ISL: Indian SL, RWTH-PHOENIX: German SL Dataset.

without creating segments in manually is a very difficult task Ibrahim et al., (2020) [14]. This issue gets even more complicated by variations in speed of signing between different individuals, expression, and regional styles Sarhan et al. (2023) [19], Saunders et al. (2022) [24].

C. Generalization to Unseen Signers and Environments

One if the major constraints for the Models is that they are trained on a limited set of signers and they often fail to generalize in recognizing and differentiating the unseen users due to differences in hand shapes, motion patterns, body proportions, and signing styles Papastratis et al., (2021) [4]. Additionally, models trained in controlled settings like good lighting, no background clutter etc. perform less efficiently in unrestricted environments with changing backgrounds, lighting, and occlusions Najib (2025) [10].

D. Real-Time Processing and Computational Constraints

Deploying SLR systems in real-world applications such as assistive tools or mobile devices needs models which are lightweight and that can process gestures in real time with minimal or no time difference. However, high-performing models made of architectures like 3D CNNs and Transformers often demands for considerable computational resources, which is commonly not available and makes them unsuitable for edge deployment without significant optimization for real-world use Dignan et al. (2022) [3], Chen et al. (2021) [33].

E. Ethical, Cultural, and Accessibility Considerations

SLR systems must be compatible to the cultural diversity in sign languages as gestures, grammars, syntax, signs all can vary widely across regions. For example, the authors take Indian sign Language is Completely contrasting in sign gestures, and grammar from American sign language, so a model specifically trained on American Sign Language (ASL), is not transferable to Indian Sign

Received: June 11, 2025. Reviewed: November 23, 2025. Accepted: December 9, 2025.

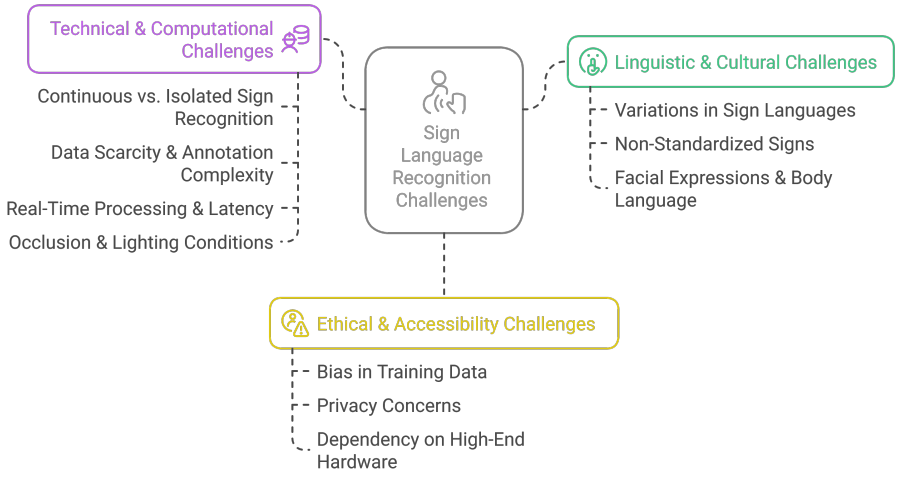

Fig. 8: Challenges and Limitations of Sign Language Recognition

Language (ISL) or British Sign Language (BSL). Moreover, most of the datasets does not consider the representation from disabled, elderly, or non-native signers which can further lead to inefficiency when they try to use it, all these raise concerns about fairness and accessibility Hussain et al. (2023) [15]. There are also privacy and ethical issues about the collection of video data, footage or real- time video capture for training, what if the data is collected without consent Adeyanju et al. (2021) [6]. The Figure 9 shows the Ethical, Cultural, and Accessibility Considerations in sign language recognition.

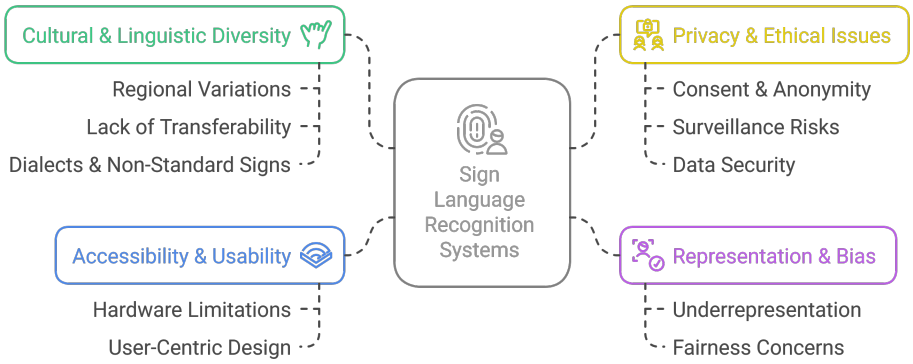

Fig. 9: Ethical and Cultural Considerations in SLR Systems

IV. Future Directions and Research Opportunities

As sign language recognition systems are continuously evolving, there are many promising directions for future research and scopes. The main motive of these scopes is to overcome existing limitations, to enhance model generalizability, accessibility and real time implementation without constraints. The Figure 10 shows the Future Directions and Research Opportunities in sign language recognition.

Received: June 11, 2025. Reviewed: November 23, 2025. Accepted: December 9, 2025.

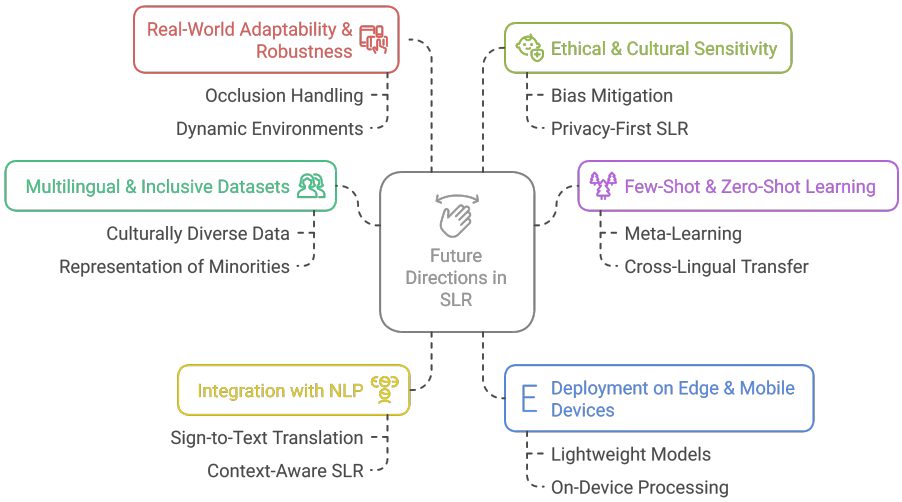

Fig. 10: Future Directions and Research Opportunities in SLR

A. *Expansion of Multilingual and Inclusive Datasets*

An important step toward creating better SLR systems is the creation of larger, multilingual, and demographically diverse datasets for model training. Future datasets should include signers of various ages, abilities, and physical conditions to guarantee fair, accessible and inclusive models. Additionally, some languages that majorly lacks annotated datasets such as African, Southeast Asian, and indigenous sign languages should be considered to annotate as they are largely unexplored Madhiarasan and Roy (2022) [2], Subburaj and Murugavalli (2022) [12], Hussain et al. (2023) [15], Joze et al. (2018) [27], Albanie et al.(2020) [28], Li, Y., Zhang et al. (2022) [29], Papadimitriou et al.(2024) [30].

B. *Few-Shot and Zero-Shot Learning Approaches*

To remove the dependency of models on large annotated datasets, future models can try adopting the few-shot and zero-shot learning paradigms. These approaches work on the simple strategy i.e. to recognize new gestures or signs with minimal possible or no training data. Combining this with techniques like meta-learning and contrastive learning can help our models to generalize to unseen sign classes with better efficiency as per the current level Adeyanju et al. (2021) [6], Najib (2025) [10] Kadam et al. (2020) [25].

C. *Integration with Natural Language Processing (NLP)*

As our current SLR systems can translate signs to individual words or phrases, future research can also focus on context-aware sentence generation using advanced NLP models. Embedding syntactic and grammatical analysis can allow systems to produce natural, grammatically correct output, which will enhance their practical use in real-time translation tools Bhaumik et al. (2023) [9], Najib (2025) [10], Nadkarni et al. (2011) [20], Kumar et al. (2023) [21].

D. *Deployment on Edge and Mobile Devices*

Developing models that are lightweight and efficient which can be deployed on smartphones, AR glasses, and other edge devices without any specific system requirements is a key research direction. Optimizing the already available deep learning models using pruning, quantization, and knowledge distillation techniques will play crucial role in achieving real-time translation of Sign Language without depending on cloud infrastructure Papastratis et al., (2021) [4], Najib (2025) [10].

Received: June 11, 2025. Reviewed: November 23, 2025. Accepted: December 9, 2025.

E. Real-World Adaptability and Robustness

Models that are to be trained and evaluated should be trained under real-world conditions, such as different lighting condition, occlusions, and complex backgrounds which will help in training the model that provides better efficiency. Furthermore, adaptive models that can learn from user feedback and self-correct in dynamic environments can be implemented to improve long-term usability and reliability Dignan et al. (2022) [3], Ibrahim et al., (2020) [14].

F. Ethical and Cultural Sensitivity in Model Design

As Sign Language Recognition systems are being deployed more widely, developers must not compromise with the cultural, ethical, and accessibility considerations in their design or datasets. This includes respecting the linguistic identity of Deaf communities, ensuring privacy in data collection, and adding sign language users in the development cycle of the model and datasets as well to co-design inclusive technologies Hussain et al. (2023) [15], Adeyanju et al. (2021) [6].

V. Conclusion

This review paper provides a comprehensive discussion about Technologies used in Artificial Intelligence (AI) based Sign Language Recognition Systems, particularly about Machine Learning and Deep Learning approaches. From early classical machine learning models to deep learning models including CNNs, LSTMs, 3D-CNNs, Spatiotemporal models and real-time and lightweight model with MobileNet, the field has taken significant steps in improving gesture recognition, translation accuracy and accessibility for the users Alzubaidi et al. (2021) [31], Al-Selwi et al. (2024) [32], Chen et al. (2021) [33], Nadkarni et al. (2011) [20], Kumar et al. (2023) [21], Kadam et al. (2020) [25]. The comparative analysis shows that video-based inputs and Continuous Sign Language Recognition (CSLR) have become the preferred choice of research and development due to their ability to capture dynamic gestures and real-time interaction. Models like R(2+1)D CNNs, CNN-LSTM hybrids, and attention-based transformers have achieved notable accuracy, especially when trained in vast and diverse datasets. Despite all the achievements these systems remain highly influenced by the quality of datasets, signer variability, and deployment constraints. Apart from these, the major challenges that stays persistent are data scarcity for low-resource sign language, generalizability for unseen signers and real-time processing limitations. Looking ahead, AI-based Sign Language Recognition System holds tremendous amount of potential with real-time lightweight models, few-shot learning techniques and integration with NLP and TTS technologies.

VI. Funding and Conflicts of Interest

- This study was conducted without any financial support from external funding agencies or organizations.
- The researchers involved in this work have no competing interests or financial affiliations to declare that might influence the research findings or their interpretation.

References

[1] D. Tran, H. Wang, L. Torresani, J. Ray, Y. LeCun, and M. Paluri, "A closer look at spatiotemporal convolutions for action recognition," in *Proceedings of the IEEE Conference on Computer Vision and Pattern Recognition*, 2018, pp. 6450–6459.

[2] M. Madhiarasan and P. P. Roy, "A comprehensive review of sign language recognition: Different types, modalities, and datasets," *arXiv preprint arXiv:2204.03328*, 2022.

[3] C. Dignan, E. Perez, I. Ahmad, M. Huber, and A. Clark, "An AI-based approach for improved sign language recognition using multiple videos," *Multimedia Tools and Applications*, vol. 81, no. 24, pp. 34525–34546, 2022. DOI: 10.1007/s11042-022-13076-8.

[4] I. Papastratis, C. Chatzikonstantinou, D. Konstantinidis, K. Dimitropoulos, and P. Daras, "Artificial intelligence technologies for sign language," *Sensors*, vol. 21, no. 17, p. 5843, 2021. DOI: 10.3390/s21175843.

[5] A. Vaswani, N. Shazeer, N. Parmar, J. Uszkoreit, L. Jones, A. N. Gomez, Ł. Kaiser, and I. Polosukhin, "Attention is all you need," *Advances in Neural Information Processing Systems*, vol. 30, 2017.

[6] I. A. Adeyanju, O. O. Bello, and M. A. Adegboye, "Machine learning methods for sign language recognition: A critical review and analysis," *Intelligent Systems with Applications*, vol. 12, p. 200056, 2021. DOI: 10.1016/j.iswa.2021.200056.

[7] K. Amrutha and P. Prabu, "ML based sign language recognition system," in *2021 International Conference on Innovative Trends in Information Technology (ICITIIT)*, 2021, pp. 1–6. DOI: 10.1109/ICITIIT51526.2021.9399601.

Received: June 11, 2025. Reviewed: November 23, 2025. Accepted: December 9, 2025.

[8] O. A. Oyeniran, J. O. Oyeniyi, K. A. Sotonwa, and A. O. Ojo, "Review of the application of artificial intelligence in sign language recognition system," *International Journal of Engineering and Artificial Intelligence*, vol. 1, no. 4, pp. 20–25, 2020.

[9] R. Bhaumik, S. Patra, D. Chakraborty, S. Basack, P. Mazumder, and P. Das, "Sign Language Detection and Translation," *Journal of Mines, Metals and Fuels*, pp. 607–613, 2023.

[10] F. M. Najib, "Sign language interpretation using machine learning and artificial intelligence," *Neural Computing and Applications*, vol. 37, no. 2, pp. 841–857, 2025. DOI: 10.1007/s00521-024-09884-8.

[11] A. Sultan, W. Makram, M. Kayed, and A. A. Ali, "Sign language identification and recognition: A comparative study," *Open Computer Science*, vol. 12, no. 1, pp. 191–210, 2022. DOI: 10.1515/comp-2022-0241.

[12] S. Subburaj and S. Murugavalli, "Survey on sign language recognition in context of vision-based and deep learning," *Measurement: Sensors*, vol. 23, p. 100385, 2022. DOI: 10.1016/j.measen.2022.100385.

[13] A. V. Nair and V. Bindu, "A review on Indian sign language recognition," *International Journal of Computer Applications*, vol. 73, no. 22, 2013.

[14] N. B. Ibrahim, H. H. Zayed, and M. M. Selim, "Advances, challenges and opportunities in continuous sign language recognition," *Journal of Engineering and Applied Sciences*, vol. 15, no. 5, pp. 1205–1227, 2020.

[15] A. Hussain, N. Saikia, and C. Dev, "Advancements in Indian sign language recognition systems: Enhancing communication and accessibility for the deaf and hearing impaired," *Asian Journal of Electrical Sciences*, vol. 12, no. 2, pp. 37–49, 2023.

[16] H. J. Hoffman, C. M. Li, K. E. Bainbridge et al., "Voice, speech, and language problems in the U.S. pediatric population: The 2012 National Health Interview Survey (NHIS)," *International Journal of Epidemiology*, vol. 44, p. i260, 2015. DOI: 10.1093/ije/dyv096.273.

[17] A. Joshi, R. Mohanty, M. Kanakanti, A. Mangla, S. Choudhary, M. Barbate, and A. Modi, "iSign: A Benchmark for Indian Sign Language Processing," *arXiv preprint arXiv:2407.05404*, 2024.

[18] N. Aloysius and M. Geetha, "Understanding vision-based continuous sign language recognition," *Multimedia Tools and Applications*, vol. 79, no. 31, pp. 22177–22209, 2020. DOI: 10.1007/s11042-020-09169-x.

[19] N. Sarhan and S. Frintrop, "Unraveling a decade: a comprehensive survey on isolated sign language recognition," in *Proceedings of the IEEE/CVF International Conference on Computer Vision*, 2023, pp. 3210–3219. DOI: 10.1109/ICCV51070.2023.00300.

[20] P. M. Nadkarni, L. Ohno-Machado, and W. W. Chapman, "Natural language processing: an introduction," *Journal of the American Medical Informatics Association*, vol. 18, no. 5, pp. 544–551, 2011. DOI: 10.1136/amiajnl-2011-000464.

[21] Y. Kumar, A. Koul, and C. Singh, "A deep learning approaches in text-to-speech system: a systematic review and recent research perspective," *Multimedia Tools and Applications*, vol. 82, no. 10, pp. 15171–15197, 2023. DOI: 10.1007/s11042-023-15489-5.

[22] M. Al-Qurishi, T. Khalid, and R. Souissi, "Deep learning for sign language recognition: Current techniques, benchmarks, and open issues," *IEEE Access*, vol. 9, pp. 126917–126951, 2021. DOI: 10.1109/ACCESS.2021.3110912.

[23] W. Wang, Y. Li, T. Zou, X. Wang, J. You, and Y. Luo, "A novel image classification approach via dense-MobileNet models," *Mobile Information Systems*, vol. 2020, p. 7602384, 2020. DOI: 10.1155/2020/7602384.

[24] B. Saunders, N. C. Camgoz, and R. Bowden, "Signing at scale: Learning to co-articulate signs for large-scale photo-realistic sign language production," in *Proceedings of the IEEE/CVF Conference on Computer Vision and Pattern Recognition*, 2022, pp. 5141–5151. DOI: 10.1109/CVPR52688.2022.00508.

[25] S. Kadam and V. Vaidya, "Review and analysis of zero, one and few shot learning approaches," in *Intelligent Systems Design and Applications*, 2020, pp. 100–112. DOI: 10.1007/978-3-030-16657-1_10.

[26] A. Sridhar, R. G. Ganesan, P. Kumar, and M. Khapra, "Include: A large-scale dataset for indian sign language recognition," in *Proceedings of the 28th ACM International Conference on Multimedia*, 2020, pp. 1366–1375. DOI: 10.1145/3394171.3413528.

[27] H. R. V. Joze and O. Koller, "Ms-asl: A large-scale data set and benchmark for understanding american sign language," *arXiv preprint arXiv:1812.01053*, 2018.

[28] S. Albanie, G. Varol, L. Momeni, T. Afouras, J. S. Chung, N. Fox, and A. Zisserman, "BSL-1K: Scaling up co-articulated sign language recognition using mouthing cues," in *Computer Vision–ECCV 2020*, 2020, pp. 35–53. DOI: 10.1007/978-3-030-58580-8_3.

[29] Y. Li, Y. Zhang, Z. Zhao, L. Shen, W. Liu, W. Mao, and H. Zhang, "CSL: A large-scale Chinese scientific literature dataset," *arXiv preprint arXiv:2209.05034*, 2022.

[30] K. Papadimitriou, G. Sapountzaki, K. Vasilaki, E. Efthimiou, S. E. Fotinea, and G. Potamianos, "A large corpus for the recognition of Greek Sign Language gestures," *Computer Vision and Image Understanding*, vol. 249, p. 104212, 2024. DOI: 10.1016/j.cviu.2024.104212.

Received: June 11, 2025. Reviewed: November 23, 2025. Accepted: December 9, 2025.

[31] L. Alzubaidi, J. Zhang, A. J. Humaidi, A. Al-Dujaili, Y. Duan, O. Al-Shamma, J. Santamaría, M. A. Fadhel, M. Al-Amidie, and L. Farhan, "Review of deep learning: concepts, CNN architectures, challenges, applications, future directions," *Journal of Big Data*, vol. 8, no. 1, p. 53, 2021. DOI: 10.1186/s40537-021-00444-8.

[32] S. M. Al-Selwi, M. F. Hassan, S. J. Abdulkadir, A. Muneer, E. H. Sumiea, A. Alqushaibi, and M. G. Ragab, "RNN-LSTM: From applications to modeling techniques and beyond—Systematic review," *Journal of King Saud University-Computer and Information Sciences*, vol. 36, no. 2, p. 102068, 2024. DOI: 10.1016/j.jksuci.2024.102068.

[33] C. F. R. Chen, R. Panda, K. Ramakrishnan, R. Feris, J. Cohn, A. Oliva, and Q. Fan, "Deep analysis of CNN-based spatio-temporal representations for action recognition," in *Proceedings of the IEEE/CVF Conference on Computer Vision and Pattern Recognition*, 2021, pp. 6165–6175. DOI: 10.1109/CVPR46437.2021.00610.

[34] V. Uniyal, S. Panchpuri, and G. Kamboj, "A Survey of Privacy-Handling Techniques and Algorithms for Data Mining," *HCTL Open International Journal of Technology Innovations and Research*, vol. 8, 2014. ISBN: 978-1-62951-499-4.

[35] V. Uniyal, S. Panchpuri, and G. Kamboj, "A Survey of Security Techniques and Algorithms for Data Mining," *HCTL Open International Journal of Technology Innovations and Research*, vol. 8, 2014. ISBN: 978-1-62951-499-4.

[36] S. Joshi, R. Shah, Y. Chandola, and V. Uniyal, "Classification of Brain MRI Images using End-to-end Trained AlexNet & End-to-end Pre-trained MobileNet," *International Journal of Research Publication and Reviews*, vol. 5, no. 7, pp. 205–218, 2024.

[37] Y. Chandola, V. Uniyal, Y. Bachheti, N. Lakhera, and R. Rawat, "Data Augmentation Techniques Applied to Medical Images," *International Journal of Research Publication and Reviews*, vol. 5, no. 7, pp. 483–501, 2024.

[38] Y. Chandola, V. Uniyal, R. Rawat, and A. Dhaundiyal, "Transformative Impact of Cloud Computing on the Gaming Industry," *International Journal of Research Publication and Reviews*, vol. 5, no. 7, pp. 465–482, 2024.

[39] Y. Chandola, J. Virmani, H. S. Bhadauria, and P. Kumar, *Deep Learning for Chest Radiographs: Computer-Aided Classification*. Elsevier, 2021. ISBN: 9780323901840.

[40] Y. Chandola, J. Virmani, H. Bhadauria, and P. Kumar, "Introduction," in *Deep Learning for Chest Radiographs*, 2021, pp. 1–33. DOI: 10.1016/B978-0-323-90184-0.00003-5.

[41] Y. Chandola, J. Virmani, H. Bhadauria, and P. Kumar, "Review of related work," in *Deep Learning for Chest Radiographs*, 2021, pp. 35–57. DOI: 10.1016/B978-0-323-90184-0.00010-2.

[42] Y. Chandola, J. Virmani, H. Bhadauria, and P. Kumar, "Methodology adopted for designing of computer-aided classification systems for chest radiographs," in *Deep Learning for Chest Radiographs*, 2021, pp. 59–115. DOI: 10.1016/B978-0-323-90184-0.00008-4.

[43] Y. Chandola, J. Virmani, H. Bhadauria, and P. Kumar, "End-to-end pre-trained CNN-based computer-aided classification system design for chest radiographs," in *Deep Learning for Chest Radiographs*, 2021, pp. 117–140. DOI: 10.1016/B978-0-323-90184-0.00011-4.

[44] Y. Chandola, J. Virmani, H. Bhadauria, and P. Kumar, "Hybrid computer-aided classification system design using end-to-end CNN-based deep feature extraction and ANFC-LH classifier for chest radiographs," in *Deep Learning for Chest Radiographs*, 2021, pp. 141–156. DOI: 10.1016/B978-0-323-90184-0.00007-2.

[45] Y. Chandola, J. Virmani, H. Bhadauria, and P. Kumar, "Hybrid computer-aided classification system design using end-to-end Pre-trained CNN-based deep feature extraction and PCA-SVM classifier for chest radiographs," in *Deep Learning for Chest Radiographs*, 2021, pp. 157–166. DOI: 10.1016/B978-0-323-90184-0.00005-9.

[46] Y. Chandola, J. Virmani, H. Bhadauria, and P. Kumar, "Lightweight end-to-end Pre-trained CNN-based computer-aided classification system design for chest radiographs," in *Deep Learning for Chest Radiographs*, 2021, pp. 167–183. DOI: 10.1016/B978-0-323-90184-0.00001-1.

[47] Y. Chandola, J. Virmani, H. Bhadauria, and P. Kumar, "Hybrid computer-aided classification system design using lightweight end-to-end Pre-trained CNN-based deep feature extraction and ANFC-LH classifier for chest radiographs," in *Deep Learning for Chest Radiographs*, 2021, pp. 185–196. DOI: 10.1016/B978-0-323-90184-0.00009-6.

[48] Y. Chandola, J. Virmani, H. Bhadauria, and P. Kumar, "Hybrid computer-aided classification system design using lightweight end-to-end Pre-trained CNN-based deep feature extraction and PCA-SVM classifier for chest radiographs," in *Deep Learning for Chest Radiographs*, 2021, pp. 197–204. DOI: 10.1016/B978-0-323-90184-0.00006-0.

[49] Y. Chandola, J. Virmani, H. Bhadauria, and P. Kumar, "Comparative analysis of computer-aided classification systems designed for chest radiographs: Conclusion and future scope," in *Deep Learning for Chest Radiographs*, 2021, pp. 205–209. DOI: 10.1016/B978-0-323-90184-0.00004-7.

Received: June 11, 2025. Reviewed: November 23, 2025. Accepted: December 9, 2025.

Article

Predictive Analytics for Student Engagement in E-Learning Systems

Yerkebulan Murattaly [1] and Azamat Serek* [2]

[1]Department of Computer Science, SDU University, Kaskelen, Kazakhstan
[2]Astana IT University, Astana, Kazakhstan

DOI: 10.47344/88c0mc52

Abstract

To increase the success of students' education, it is important to be able to predict the level of their involvement in the online educational environment. This study uses the Open University Learning Analytics (OULAD) open dataset to develop a systematic and reproducible approach to classifying student engagement. On the other hand, many other studies depend on specific datasets or limited definitions of engagement. A full cycle of data preprocessing and feature extraction was implemented, aimed at obtaining informative behavioral indicators based on click data and evaluation results. We trained and tested two traditional supervised machine learning model, Random Forest and Logistic Regression, using weight and macro-average metrics. The random forest model demonstrated high efficiency across all interaction classes and showed higher accuracy (0.926) compared to logistic regression (0.896). The results obtained emphasize the importance of high-quality data preprocessing and thoughtful design of features. In addition, they confirm that such signs provide valuable information for the development of early warning systems and the further development of educational analytics in higher education institutions.

Keywords: student engagement, learning analytics, feature engineering, preprocessing pipelines, classical machine learning, Logistic Regression, Random Forest, OULAD

I. Introduction

The rapid development of online and high-tech educational environments has significantly changed modern education. Learning management systems and virtual learning environments, widely used in distance learning, is now an integral element of both fully online and blended learning models [14]. With the growing popularity of such platforms, it is becoming especially important for educational institutions to understand and monitor the level of student engagement, as well as to monitor academic performance, re-education, and course completion [15], [16]. Student engagement, usually determined by the level of attention, activity, and effort expended in the learning process, is widely considered in scientific research as a reliable indicator of the effectiveness of the educational process [3], [17], [18].

Email (1): 221107028@stu.sdu.edu.kz ORCID: 0009-0006-1210-6015
*Corresponding author:
Email: Azamat.Serek@astanait.edu.kz ORCID: 0000-0001-7096-6765

Received: December 28, 2025. Reviewed: December 29, 2025. Accepted: December 30, 2025.

Modern advances in learning analytics have made it possible to systematically analyze student interaction logs, assessment data, and behavioral patterns recorded in virtual learning environments (VLE). These datasets offer numerous opportunities for building predictive models, but because they are multidimensional, sparse, and heterogeneous, they require preprocessing to create useful features. As a result of high-quality processing of the source data from the LMS system, they are transformed into important features that increase the interpretability of models, predictive accuracy and reproducibility of results. As a result, the reliability of predicting the level of involvement of students increases. [2], [4].

An open data collection called Open University Learning Analytics (OULAD) was used to stimulate work in the field of research. This data set contains demographic data, assessment results and detailed log files reflecting their activities in the educational process in relation to 32,593 students who have completed 22 training courses. The total amount of data is more than 10.6 million activity records per day. Such a large and informative data set makes it particularly effective for forecasting tasks.g [1].

In this study, we examined five supervised machine learning algorithms—random forest (RF), gradient boosting (GB), AdaBoost, logistic regression (LR), and support vector machines (SVM) to classify student engagement levels. For a more in-depth study, we chose logistic regression and random forest because they are highly accurate, stable, and easy to understand. This choice allowed us to systematically compare the models, highlighting the importance of conducting accurate comparative analysis and obtaining consistent results.

This paper presents three main scientific contributions: (1) developing an integrated feature engineering and data preprocessing methodology for engagement prediction using OULAD behavioral data; (2) evaluating the performance of two well-known supervised learning models: random forest and logistic regression; and (3) empirically demonstrating the most important features and algorithms for engagement classification. By focusing on data preprocessing procedures and using traditional machine learning models, the results provide a replicable framework and valuable recommendations for developing early warning systems and improving educational analytics in higher education institutions.

II. Literature Review

Recently, researchers have paid special attention to student engagement in online learning, as it is directly related to academic achievement, student retention, and course completion [15], [17]. Despite the growing popularity of this topic, many unanswered questions remain regarding how to measure engagement, how to select factors for evaluation, and how to make accurate predictions based on log data from educational platforms [16]. In addition to summarizing the findings of previous studies, this review highlights the crucial role of data preprocessing and feature generation in predicting student engagement.

A. Definitions and Aspects of Engagement in E-Learning

Digital learning engagement among students is a complicated and a multidimensional issue. There are various opinions in terms of the effect on digital learning in education. There can be various possibilities what will be results of such kind of education. The majority of learning analytics research in higher education is based on observable behavioral indicators such clicks, task completion time, and login frequency, whereas the cognitive, social, and emotional aspects of engagement are frequently overlooked. Observable features are used because it can be easier to get them and analyse thereafter, Although log data provides a more convenient way to quantify behavioral engagement, this constraint restricts the efficacy of engagement models and the depth of understanding of student participation [16].

Diversity and ambiguity in terminology, measurement methods, and annotation criteria across multiple studies and datasets have been identified in recent reviews of automated engagement assessment [8], [9], [16]. Currently diversification is undergoing increase. Only a few of them correlate with validated psychological scales, which makes it difficult for cross-study comparisons and generalization of results [15], [17]. In this regard, the importance of using frameworks that cover the behavioral, cognitive, social, and emotional aspects of engagement is emphasized, as well as the need for careful data preprocessing to transform heterogeneous log data into informative signs of interaction [17]. These frameworks highlight the importance of preprocessing: changing mixed raw data into clear and meaningful features that capture different parts of the engagement. Preprocessing is also very important in terms of subsequent machine learning application because the data should be clean before we actually apply machine learning.

B. Practical Application of Learning Analytics for Engagement or Performance Forecasting

Research based on online learning data aims to predict the level of engagement and learning outcomes of students. Early work has shown that predictive models that take into account behavioral, collaborative, and emotional components can serve as an early

Received: December 28, 2025. Reviewed: December 29, 2025. Accepted: December 30, 2025.

warning system [5]. Other studies focus on analyzing behavioral interactions in self-regulated and survey-oriented online modules, including interaction with content, duration of activity, and resources used, demonstrating a close relationship between behavioral traits and learning outcomes and engagement levels.

The consistency and sustainability of the engagement metrics extracted from LMS journals have a huge impact on academic performance, and machine learning models trained on such data that usually demonstrate high predictive accuracy [16]. Developing multimodal approaches by combining the analysis of gaze, facial expressions and actions shows that the integration of visual and behavioral data makes it possible to more accurately assess engagement compared to using a single source of information [17]. At the same time, the majority of studies emphasize that the quality of data preprocessing and feature development directly determines the accuracy of forecasting and interpretability of models.

C. Challenges, Limitations, and Gaps in Existing Research

Despite the progress made, there are still a number of challenges in this area. Many studies focus primarily on behavioral indicators, while the cognitive and emotional aspects of the engagement remain insufficiently considered [5], [15]. Approaches to defining interaction protocols and annotations are inconsistent, and the use of validated scales is found only in a limited number of papers [8], [16], [17]. Large publicly available datasets are used relatively rarely, which reduces the possibility of generalizing the results and reproducibility of research. Comparative studies of classical supervised machine learning algorithms are also insufficient, which makes it difficult to identify sustainably effective methods. In addition, works devoted to replication and comparative analysis are rare due to the variety of data sets and methodological approaches used, and the stages of data preprocessing are often described superficially, which limits the reproducibility and practical applicability of engagement forecasting models.

D. Implications for the Current Study and Knowledge Deficiency

The literature emphasizes that predicting engagement is a dynamically developing field, but most research is limited to rigid definitions, inconsistent indicators, and the use of specialized or small datasets. In this regard, there is an obvious need for systematic research based on large publicly available data, the use of supervised machine learning methods and clearly described procedures for preprocessing and feature development [8].

Using the Open University Learning Analytics (OULAD) dataset and extracting meaningful behavioral characteristics through a rigorous data preparation cycle, this work fills these gaps. Due to their high predictive performance, interpretability, and robustness, logistic regression and random forest were selected for further investigation. By highlighting the critical role of data preprocessing in obtaining consistent and understandable results, the proposed methodology establishes a replicable standard and provides empirical evidence for the effectiveness of traditional engagement prediction algorithms [5].

III. Methods

This section showcases the methods that we used and the methodology to achieve research aim that we outlined in the introduction section.

A. Dataset Description and Rationale

This work utilized open source dataset. The study used the Open University Learning Analytics (OULAD) dataset, which includes complete log-records describing student demographic characteristics, course metadata, evaluation metrics, and virtual learning environment (VLE) activities [21].

Figure 1 showcases the snippet of the dataset that was used in our experiments.

B. Data Cleaning, Integration, and Feature Engineering

Before the application of machine learning, it is quite important to make preprocessing. Because without preprocessing, the data will not undergo the required changes and the results might become biased or improper. Firstly, we dealt with missing values in the dataset. We handled missing values of features based on their data types in the dataset. Because if the data type is string (text), then it will have another strategy rather than if the data type of the feature was integer. For instance, we used the mode for categorical features, whereas for numerical features we used median value as a replacement. We set unsubmitted assessment scores to zero. To show that someone did not withdraw, missing unregistration dates were given a value of -1. We used features of id student, code

Received: December 28, 2025. Reviewed: December 29, 2025. Accepted: December 30, 2025.

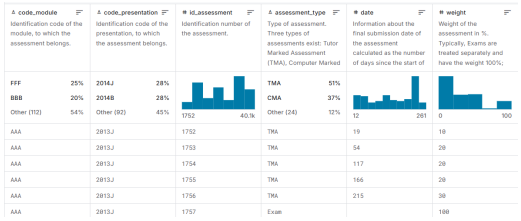

Fig. 1: Snippet of dataset.

module, and code presentation to combine the tables. As a result, we put together features as total and average assessment scores, total VLE clicks, normalized clicks per credit, and score per assessment. Other engineered features are the time between registration and the start of a module and the length of time a person can participate.

C. Train-Test Partitioning

Division of the dataset into train and test is very important. Because even if the accuracy is high in training, it does not mean that the accuracy will be high in testing part. The 80/20 stratified split was applied to preserve class distribution for classification tasks. Stratification ensures reliable performance estimate by preventing over or under presence of any class. Two main models were used in the work: logistic regression and random forest. At the initial stage, five classical algorithms were considered: LR, RF, Gradient Boosting, AdaBoost, and the support vector machine method. LR and RF were selected for further analysis, as they demonstrated a higher quality of forecasting, better interpretability and stability of the results.

D. Models

This section explains the models that we used in our study with corresponding justification of uses. To train logistic regression, a stratified 5-fold cross-validation was used with the adjustment of hyperparameters C and solver. The evaluation metrics used were macro-accuracy, macro-completeness, macro F1-measure, and accuracy. Confusion matrices were visualized using the `seaborn` library for visual analysis of the results. Logistic regression served as a transparent linear basic model reflecting the general patterns of engagement levels. An accelerated workflow based on `RandomizedSearchCV` was used to train the random forest model. This approach sampled a smaller number of hyperparameter combinations across `n_estimators`, `max_depth`, `min_samples_split`, `min_samples_leaf`, `max_features`, and `bootstrap`. In order to reduce the calculation time and increase the generalizability of the results, a stratified triple cross-validation was used. The same metrics were used for estimation as for logistic regression, and confusion matrices were visualized using `Matplotlib`. This approach simplified the configuration of the model and allowed us to take into account non-linear interactions and a complex data structure. The quality of the model was assessed by accuracy, macro-average values of completeness and F1-measure, and the analysis of confusion matrices allowed us to determine the nature of the forecast errors for each class. The combination of these indicators provided a comprehensive assessment of the effectiveness of the model in predicting the level of student engagement.

IV. Results and Discussion

This section showcases obtained results and the discussion of what we found with corresponding analysis of strengths and weaknesses of our obtained results. To make hyperparameter tuning we applied grid search. It was applied to aim to get optimal values for hyperparameters of the applied models. The logistic regression model was configured using a grid search to determine optimal hyperparameter values:

```
C = 1, solver = 'liblinear'
```

The performance indicators of the logistic regression model are shown in table I. The overall accuracy of the model was determined at 0.896, while the macro-average indicators of accuracy, completeness and F1 dimensions were also approximate to this value. The classification report (Table II)indicates balanced results for both classes.

Received: December 28, 2025. Reviewed: December 29, 2025. Accepted: December 30, 2025.

TABLE I: Evaluation Metrics (Weighted & Macro) of Logistic Regression

Metric	Score
Accuracy	0.8957
Precision (Macro)	0.8959
Recall (Macro)	0.8972
F1-score (Macro)	0.8956

TABLE II: Classification Report of Logistic Regression

Class	Precision	Recall	F1-score	Support
0	0.93	0.87	0.90	3442
1	0.86	0.92	0.89	3077
Accuracy			0.90	
Macro Avg	0.90	0.90	0.90	6519
Weighted Avg	0.90	0.90	0.90	6519

The results show that logistic regression provides a fairly accurate classification of student engagement, demonstrating a slight improvement in completeness for class 1 and a slight increase in accuracy for class 0. The following optimal hyperparameter values were determined for the random forest model (accelerated version):

```
n_estimators = 160, min_samples_split = 10, min_samples_leaf = 3,
max_features = None, max_depth = 15, bootstrap = True
```

In general, the random forest model surpassed the logistic regression, reaching an accuracy of 0.926. The macro-averaged values of accuracy, completeness, and F1-measure also amounted to about 0.926 (Table III). The classification report presented in IVshows stable performance of the model in both classes, with a slight increase in accuracy for class 1 and completeness for class 0 compared to logistic regression.

TABLE III: Random Forest Performance Metrics

Metric	Score
Accuracy	0.9262
Precision (Macro)	0.9265
Recall (Macro)	0.9278
F1-score (Macro)	0.9262

TABLE IV: Random Forest Classification Report

Class	Precision	Recall	F1-score	Support
0	0.96	0.90	0.93	3442
1	0.90	0.96	0.92	3077
Accuracy			0.93	
Macro Avg	0.93	0.93	0.93	6519
Weighted Avg	0.93	0.93	0.93	6519

The findings demonstrate that Random Forest, employing an ensemble-based approach, markedly improves both accuracy and class performance equilibrium in comparison to Logistic Regression. This study did not examine additional algorithms such as Gradient Boosting, AdaBoost, and Support Vector Machines, as the integration of Logistic Regression and Random Forest demonstrated significant efficacy and sufficient benchmarking for traditional supervised methods. We could focus on making sure our results could be repeated, that our models were easy to understand, and that we were using well-known metrics for a strong comparison

Received: December 28, 2025. Reviewed: December 29, 2025. Accepted: December 30, 2025.

with this method. We created confusion matrices for both Logistic Regression (Figure 1) and Random Forest (Figure 2) to see how well the models worked. These matrices show in great detail how well each model groups students based on how interested they are. The confusion matrix shows that Logistic Regression worked about the same for both classes. Of the 3442 students who were either low-engaged or failed, 93 percent were correctly classified, and 7 percent were incorrectly classified as high-engaged or passed. In the high-engagement/pass category, 86% were accurately identified, whereas 14% were erroneously predicted to exhibit low engagement/failure. This pattern shows that Logistic Regression does a good job of finding overall trends, but it does show a slightly higher rate of false negatives in the high-engagement group.

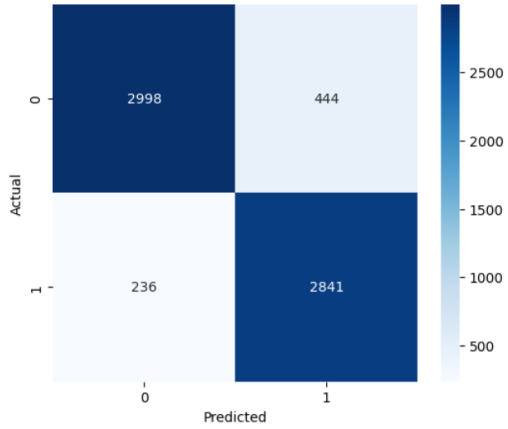

Fig. 2: Confusion matrix for Logistic Regression.

The Random Forest confusion matrix shows that it can now classify things much better. Ninety-six percent of the time, students who did not participate or failed were correctly identified. Ninety percent of the time, students who did participate or passed were correctly identified. Both classes make fewer mistakes than Logistic Regression. This shows that the model can find complicated patterns and interactions that are not straight lines in the feature set. In general, Random Forest works better across classes and makes fewer mistakes, which is what you would expect from its higher F1-score and accuracy. These confusion matrices show how important it is to perform preprocessing and feature engineering. Both models can tell how engaged someone is by making meaningful behavioral features and making engagement signals across modules the same. The more complex, nonlinear interactions in the dataset are what make Random Forest work best.

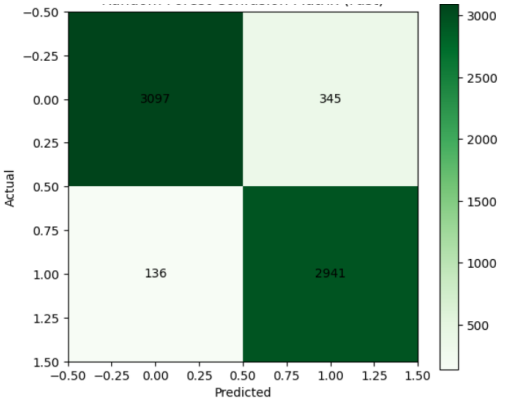

Fig. 3: Confusion matrix for Random Forest.

Received: December 28, 2025. Reviewed: December 29, 2025. Accepted: December 30, 2025.

V. Conclusions and Future Work

This study shows that classical machine learning models can effectively predict student engagement in online learning environments when used with a carefully designed preprocessing and feature engineering pipeline. We used the Open University Learning Analytics Dataset (OULAD) in order to get behavioral indicators from clickstream and assessment data, which made it easier to classify engagement in a more complete way. We looked at Logistic Regression and Random Forest, and we found that Random Forest showed better accuracy and performance in all engagement categories. These results show that traditional supervised learning methods can still be useful for predict engagement when they are used with careful preprocessing. They can also be considered as clear, repeatable standards for research in learning analytics. This study shows that the preprocessing of data and the formation of characteristic features have a decisive influence on the quality of the model. Converting the source information from the LMS system into structured capabilities will enhance the interpretation of models and increase the accuracy of forecasting. Such approach is important in the educational process for the early identification of risk groups and the development of effective training strategies. The proposed method can be adapted to various educational data sets and conditions for conducting comparative analysis. In upcoming studies, the use of time modeling, as well as the introduction of cognitive and emotional indicators obtained through questionnaires and computer vision methods, can further improve the quality of the forecast. In addition, a comparison of classical machine learning approaches with modern models of deep learning paves the way for a deeper understanding of the relationship between interpretation capability and computational complexity.

References

[1] Jakub Kuzilek, Martin Hlosta, Zdenek Zdrahal, *Open University Learning Analytics dataset*, Scientific Data, vol.4, p.170171, 2017. DOI: https://doi.org/10.1038/sdata.2017.171

[2] Khurram Jawad, Muhammad Arif Shah, Muhammad Tahir, *Students' Academic Performance and Engagement Prediction in a Virtual Learning Environment Using Random Forest with Data Balancing*, Sustainability, vol.14, no.22, p.14795, 2022. DOI: https://doi.org/10.3390/su142214795

[3] M. Yağcı, *Educational data mining: prediction of students' academic performance using machine learning algorithms*, Smart Learning Environments, vol.9, p.11, 2022. DOI: https://doi.org/10.1186/s40561-022-00192-z

[4] Zhaoyu Shou, Mingquan Xie, Jianwen Mo, Huibing Zhang, *Predicting Student Performance in Online Learning: A Multidimensional Time-Series Data Analysis Approach*, Applied Sciences, vol.14, no.6, p.2522, 2024. DOI: https://doi.org/10.3390/app14062522

[5] M. A. A. Dewan, M. Murshed F. Lin, *Engagement detection in online learning: a review*, Smart Learning Environments, vol.6, article 1, 2019. DOI: https://doi.org/10.1186/s40561-018-0080-z

[6] N. A. Johar, S. N. Kew, Z. Tasir E. Koh, *Learning Analytics on Student Engagement to Enhance Students' Learning Performance: A Systematic Review*, Sustainability, vol.15, no.10, article 7849, 2023. DOI: https://doi.org/10.3390/su15107849

[7] M. B. Garcia, C.-L. Goi, K. Shively D. Maher, *Understanding Student Engagement in AI-Powered Online Learning Platforms: A Narrative Review of Key Theories and Models*, in Cases on Enhancing P-16 Student Engagement With Digital Technologies, 2025. DOI: https://doi.org/10.4018/979-8-3693-5633-3.ch001

[8] S. S. Khan, A. Abedi T. Colella, *Inconsistencies in the Definition and Annotation of Student Engagement in Virtual Learning Datasets: A Critical Review*, arXiv preprint, 2022. URL: https://arxiv.org/abs/2208.04548

[9] S. N. Karimah et al., *Automatic engagement estimation in smart education/learning settings: a systematic review of engagement definitions, datasets, and methods*, Smart Learning Environments, vol.9, article31, 2022. DOI: https://doi.org/10.1186/s40561-022-00212-y

[10] N. J. Falkner K. E. Falkner, *Predicting Student Engagement in the Online Learning Environment*, International Journal of Web-Based Learning and Teaching Technologies, vol.16, pp.1–17, 2021. DOI: https://doi.org/10.4018/IJWLTT.287095 (sciencedirect.com)

[11] M. A. Al Mamun G. Lawrie, *Student-content interactions: Exploring behavioural engagement with self-regulated inquiry-based online learning modules*, Smart Learning Environments, vol.10, article1, 2023. DOI: https://doi.org/10.1186/s40561-022-00221-x (slejournal.springeropen.com)

[12] B. Flanagan, R. Majumdar H. Ogata, *Early-warning prediction of student performance and engagement in open book assessment by reading behavior analysis*, International Journal of Educational Technology in Higher Education, vol.19, article41, 2022. DOI: https://doi.org/10.1186/s41239-022-00348-4 (educationaltechnologyjournal.springeropen.com)

Received: December 28, 2025. Reviewed: December 29, 2025. Accepted: December 30, 2025.

[13] User667, *OULAD Personalized Learning Path*, Kaggle Notebook and Dataset, 2025. URL: https://www.kaggle.com/code/user667/oulad-personalized-learning-path

[14] P.-C. Sun, R. J. Tsai, G. Finger, Y.-Y. Chen D. Yeh, *What drives a successful e-Learning? An empirical investigation of the critical factors influencing learner satisfaction*, Computers Education, vol.50, pp.1183–1202, 2008. DOI: https://doi.org/10.1016/j.compedu.2006.11.002

[15] C. R. Henrie, L. R. Halverson C. R. Graham, *Measuring student engagement in technology-mediated learning: A review*, Computers Education, vol.90, pp.36–53, 2015. DOI: https://doi.org/10.1016/j.compedu.2015.09.005

[16] M. Bond, S. Bedenlier, V. I. Marín M. Händel, *Student engagement in blended learning environments: A review of the literature*, International Journal of Educational Technology in Higher Education, vol.17, article1, 2020. DOI: https://doi.org/10.1186/s41239-020-00214-5

[17] J. A. Fredricks, P. C. Blumenfeld A. H. Paris, *School engagement: Potential of the concept, state of the evidence*, Review of Educational Research, vol.74, pp.59–109, 2004. DOI: https://doi.org/10.3102/00346543074001059

[18] R. M. Carini, G. D. Kuh S. P. Klein, *Student engagement and student learning: Testing the linkages*, Research in Higher Education, vol.47, pp.1–32, 2006. DOI: https://doi.org/10.1007/s11162-005-8150-9

[19] Qi, Y.; Zhuang, L.; Chen, H.; Han, X.; Liang, A. *Evaluation of Students' Learning Engagement in Online Classes Based on Multimodal Vision Perspective*, Electronics, vol.13, article149, 2024. DOI: https://doi.org/10.3390/electronics13010149 (mdpi.com)

[20] Tang, X.; Gong, Y.; Xiao, Y.; Xiong, J.; Bao, L. *Facial Expression Recognition for Probing Students' Emotional Engagement in Science Learning*, Journal of Science Education and Technology, vol.34, pp.13–30, 2025. DOI: https://doi.org/10.1007/s10956-024-10143-7 (link.springer.com)

[21] Kuzilek, J., Hlosta, M. & Zdrahal, Z. Open University Learning Analytics dataset. *Scientific Data* **4**, 170171 (2017). https://doi.org/10.1038/sdata.2017.171

Received: December 28, 2025. Reviewed: December 29, 2025. Accepted: December 30, 2025.

SECTION II
Infocommunication Technologies

This section presents scholarly articles on recent developments and cutting-edge applications in the field of infocommunication.

Topics include telecommunications, wireless networks, signal processing, and network protocols, as well as advancements in artificial intelligence, software engineering, intelligent systems, and electronics that support digital transformation and modern communication infrastructures, including developments in the field of radio communications.

Article

A MULTILEVEL CONVERTER WITH TRIPLE VOLTAGE BOOST FOR RENEWABLE ENERGY SOURCES

Kyrmyzy Taissariyeva [1] and Zhansaya Ayapbergen* [2]

[1]Department of Electronics, Telecommunications and Space Technologies, Satbayev University, Almaty, Kazakhstan

[2]Department of Electronics, Telecommunications and Space Technologies, Satbayev University, Almaty, Kazakhstan

DOI: 10.47344/hxfy6e54

Abstract

A compact, single-supply, multilevel inverter (SC-MLI) topology based on a switched-capacitor structure for high-efficiency power conversion is proposed. The overall goal of the study is to develop a three-stage inverter that increases the voltage by a factor of 13 while simultaneously reducing the number of required components. As a result, the proposed design reduces circuit complexity and cost while also increasing reliability. The inverter's performance was evaluated using theoretical analysis, MATLAB/Simulink and PLECS simulations, and experimental verification. In addition, tests using a natural capacitor without a control circuit or with resistive and inductive loads confirmed the stable generation of multi-level voltage and voltage balance with additional sensors. For example, when operating in sinusoidal pulse-width modulation (SPWM) and low-level control (NLC) modes, the inverter maintained low harmonic distortion and a uniform current waveform. As a result, the system achieved a maximum efficiency of 97.2% in modeling and 95.3% experimentally. The results of this study confirm the Recommended Level 13 SC-MLI compliance for renewable energy integration and other advanced power electronics applications.

Keywords: amplifier inverter; multi-level inverters (MLI); renewable energy use; self-balancing voltage; variable capacitor (SC)

I. Introduction

The growing use of renewable energy sources [1] and high-energy-density batteries has made multilevel converters (MLCs) increasingly popular in power electronics [2]. Modern systems require high efficiency, high power density, low harmonic distortion,

Email: k.taisariyeva@satbayev.university ORCID: 0000-0002-1949-4288
*Corresponding author: z.ayapbergen@satbayev.university
Email: z.ayapbergen@satbayev.university ORCID: 0009-0002-0798-7840

Received: December 22, 2025. Reviewed: December 30, 2025. Accepted: December 30, 2025.

and stable input voltage. Due to their structural advantages, MLCs enable high-quality DC–AC conversion and are widely used in electric vehicles, microgrids, charging infrastructures, and renewable-energy-based installations [3]. However, classical methods such as CHB, NPC, and FC require a large number of semiconductor components and independent power supplies, complicating circuit design and control [4]. Switched-capacitor (SC)-based topologies offer numerous advantages, such as compactness, lightweight design, high power density, and the elimination of the need for inductors for voltage conversion. These topologies make it possible for applications like multi-channel power supplies and voltage management [5,6]. These topologies also enable voltage step-up without the use of transformers, an advantage that distinguishes them from high-frequency magnetic systems [7,8]. Furthermore, capacitors are easier to use and significantly less expensive than others because they are self-balancing. Most research papers classify SC-MLI by the number of input sources, voltage step-up, and the number of output levels [10,11]. However, voltage fluctuations and the formation of low-frequency harmonics can be affected by both continuous charging and discharging [12]. Overall, a lot of work is being done on 13-level topologies, but since they require multiple input sources and a large component count, the work is somewhat more challenging. Therefore, research initiatives are placing greater emphasis on single-power supply solutions. Similar issues arise in 9-level designs, which have fewer connectors, more auxiliary components, and higher voltage between devices, the same problems come up. This paper proposes a new SC-MLC topology that uses a single power supply consisting of 3 capacitors, 11 switches, and 3 diodes. This allows for the creation of 13 different output voltage levels. By using multiple components at each level, these designs are more efficient than other solutions. The self-balancing feature means that additional balancing circuits are not required, and the single-input structure makes the topology suitable for use in high-voltage networks. The main objective of the research is to develop and experimentally verify a compact and productive SC-MLC architecture that reduces the number of components and complexity of implementation while maintaining the required characteristics. The proposed topology was validated under both low-frequency modulation and PWM operation, and simulation results were in full agreement with experimental findings, clearly demonstrating the advantages of the proposed approach over conventional counterparts.

II. Literature Review or Related Works

Multilevel converters (MLCs) are becoming increasingly valuable as interfaces in renewable energy systems such as photovoltaic (PV) cells and wind turbines. This is because they can generate very good AC waveforms and reduce the load on the electronics caused by high voltages. Early studies focused on standard MLC topologies, including diode-limited configurations, floating capacitors, and cascaded H-bridges, which show that increasing the voltage level results in reduced harmonic distortion and improved sinusoidal output waveform quality. Furthermore, most of these topologies cannot be directly used in low-voltage renewable energy systems. As they require because they require separate DC power supplies or power transformers. Much of the research has focused on improving topologies using switched capacitors (SCs) and switched inductors, i.e., multi-level topologies to boost the DC bus voltage from low-voltage renewable sources. Hu et al. (2021) present a multilevel inverter with switched capacitors, fewer circuit components, and improved voltage scaling capabilities; however, the topology does not achieve a high voltage gain using a single input source. The proposed topology allows for increased output voltage and output levels by using fewer switches, diodes, and capacitors, which means that it can still be used in renewable energy projects. Li (2018) describes a seven-level inverter with only one phase and one DC power supply. The topology employs a set of switched capacitors to triple the input DC voltage. Furthermore, it provides capacitor voltage equalization and prevents overscaling of power switches. Hussan et al. (2023) recently demonstrated a multi-level inverter (TB-SCMLI). However, the topology requires a higher number of power components to achieve similar voltage boosting. It is described as having fewer circuit components and capacitors and self-equalizing the voltage across the switching capacitors, and is designed for renewable energy systems operating at high voltages. These studies indicate that significant improvements can be achieved by significantly reducing the use of DC sources and increasing efficiency. A comparative summary of recent switched-capacitor-based multilevel inverters is presented in Table I I.

III. Methods

The structure of a switched-capacitor multilevel inverter (SC-MLI) is shown in Figure 1. The basic structure consists of a single DC power supply, ten power switches (H_1–H_4, S_1–$S_5, and S_1$), three capacitors ($C_1, C_2, and C_3$), and three separate diodes ($D_1, D_2, and D_3$). This device can produce 13 different output voltage levels with only one DC input. By adding switched capacitors, the system can obtain a threefold the output voltage. The circuit provides energy flow from the DC power supply to both the load and the capacitors through various combinations of switches. The capacitor C_1 is charged directly with the source voltage (VDC), and the capacitors C_2 and C_3 share this voltage equally. The voltages across the capacitors are $VC_1 = VDC, VC_2 = 0.5VDC, and VC_3 = 0.5VDC$. This setup works well for boosting voltage, raising the total output voltage of the main circuit to three times the input source voltage. Here, VDC denotes the input DC source voltage.

Received: December 22, 2025. Reviewed: December 30, 2025. Accepted: December 30, 2025.

TABLE I
SUMMARY OF RELATED WORKS ON BOOSTING MULTILEVEL INVERTERS

Author(s)	Year	Key Findings	DOI
Hu et al.	2021	Proposed a switched-capacitor-based multilevel inverter with reduced circuit components and voltage boosting capability, suitable for renewable energy applications.	doi:10.1002/2050-7038.12990
Lee	2018	Developed a single-phase, single-source seven-level inverter achieving triple voltage gain with automatic capacitor voltage balancing and low switch voltage stress.	doi:10.1109/ACCESS.2018.2842182
Hussan et al.	2023	Introduced a triple-boost switched-capacitor multilevel inverter (TB-SCMLI) with reduced components and self-voltage-balancing capacitors for sustainable energy systems.	doi:10.1049/pel2.12561

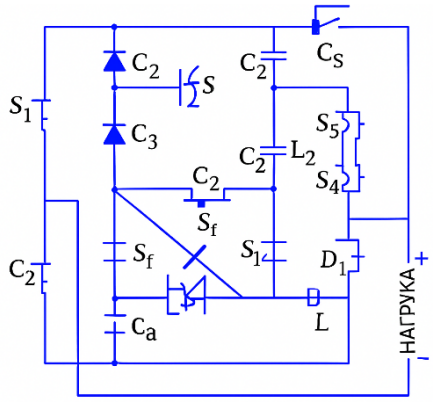

Fig. 1. Multilevel Converter with Triple Voltage Boost

The current flow channels established through the load and capacitors, corresponding to the positive, negative, and zero levels of the output voltage demonstrate the operational principle of the proposed SC-MLI architecture. The red lines representpaths of load current that occur when the capacitors discharge in different switching states. The green lines show the paths of charging current that happen when the capacitors charge. The current path analysis shows that the new SC-MLI topology can provide 13 separate output voltage levels by using only one DC source and adding the voltages of the capacitors in the right order during the right switching sequences. One of the a major challenge capacitor-based multilevel inverters (MLIs) is making sure that the voltage is evenly spread out throughout the capacitors. In many modern topologies, this requires complex control algorithms that keep a watch on capacitor voltages while they are being used. The architecture in this study allows for voltage self-balancing, therefore there is no need for extra balancing circuits or complicated control algorithms. The capacitors in this structure charge and discharge autonomously, which maintains the converter functioning smoothly without any extra systems to balance it out. However, careful selection of capacitance values is required so that the voltage doesn't shift too much. The maximum permissible discharging time (MDT) and the load current during discharging periods are two critical factors that determine the choice of capacitance. If you get the capacitance calculation right, the voltage will be stable no matter what the conditions are.

$$MDT_{C_1} = t_4 - \left(\frac{T}{2} - t_4\right)$$

$$MDT_{C_2} = MDT_{C_3} = t_5 - \left(\frac{T}{2} - t_5\right)$$

Received: December 22, 2025. Reviewed: December 30, 2025. Accepted: December 30, 2025.

During maximum discharge periods, any variation in the capacitor charge directly affects the amplitude of the output voltage ripple, as expressed in equation (1):

$$\Delta v_{C_i} = \frac{\Delta Q_{C_i}}{C_i} = \frac{1}{C_i} \int_{t_a}^{t_b} i_L \, dt$$

where Δv_{C_i} - is the voltage ripple across capacitor i during the time interval $t_a - t_b$, ΔQ_{C_i} is the amount of charge discharged to the load over this interval, and IL is the load current (which, in this case, coincides with the discharge current). The voltage drop across capacitors during the maximum discharge time (MDT) is calculated as follows [7]:

$$\Delta v_{C1} = \frac{\Delta Q_{C1}}{C_1} = \frac{1}{C_1} \int_{t_4}^{T/2-t_4} i_L \, dt$$

$$\Delta v_{C2} = \frac{\Delta Q_{C2}}{C_2} = \frac{1}{C_2} \int_{t_5}^{T/2-t_5} i_L \, dt$$

$$\Delta v_{C3} = \frac{\Delta Q_{C3}}{C_3} = \frac{1}{C_3} \int_{t_5}^{T/2-t_5} i_L \, dt$$

Since capacitor C_1 discharges within the interval $t_4 - (T/2 - t_4)$, the required capacitance for a given ripple level is determined using equation (2), derived from equations (3) and (4). Similarly, because the maximum discharge duration (MDT) for capacitors C_2 and C_3 is identical, their capacitances are calculated based on the interval $t_5 - (T/2 - t_5)$.

IV. Results and Discussion

MATLAB/Simulink and PLECS were used to create simulation models to test the performance of the proposed SC-MLI topology. To ensure reliability and comparability of results, identical circuit settings were used in both cases. The DC input voltage was set to 60 V, and the capacitance values $C_1 = 2200\,\mu$F, $C_2 = C_3 = 2200\,\mu$F were used for these theoretical calculations. The equivalent series resistance (ESR) of all capacitors was $0.08\,\Omega$. The converter was tested using near-level control (NLC) and sinusoidal pulse width modulation (SPWM) by varying the load, switching frequency, and modulation index (MI). Figure 2(a) shows the simulation results of the NLC model with three different types of loads: purely resistive $(150\,\Omega)$, resistive-inductive $(150\,\Omega + 50\,\text{mH})$, and highly inductive $(150\,\Omega + 200\,\text{mH})$. The output voltage can be varied in 13 different levels, but the current remains constant regardless of the load value. Figure 2(b) shows how the voltage ripple changes when using floating capacitors. The ripple level for each capacitor is always less than 10%. This confirms the correctness of the capacitor selection and the robustness of the proposed architecture.

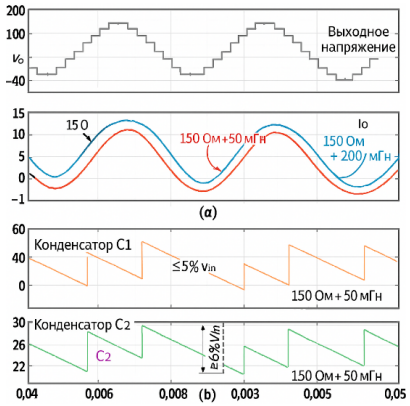

Fig. 2. (a) Output voltage and current for different load conditions; (b) Voltage ripples across capacitors

Received: December 22, 2025. Reviewed: December 30, 2025. Accepted: December 30, 2025.

The suggested SC-MLI inverter was tested again with a weakly inductive load of $(150\,\Omega + 50\,\text{mH})$, utilizing both SPWM and NLC modulation methods. Harmonic analysis was done to check the quality of the output current. Figure 3(a) shows that the current waveform achieved with SPWM control is close to the ideal sinusoidal reference for the given load conditions. The waveform generated using NLC control also exhibits adequate smoothness. Figure 3(b) shows the harmonic spectra. The total harmonic distortion (THD) of the output current was 1.36 % for SPWM and 2.21 % for NLC. The THD value is a little larger for NLC, but this approach still works because the proposed architecture creates a multilayer output voltage with a high resolution. These results show that the inverter meets the requirements for harmonic distortion without needing high-frequency modulation approaches.

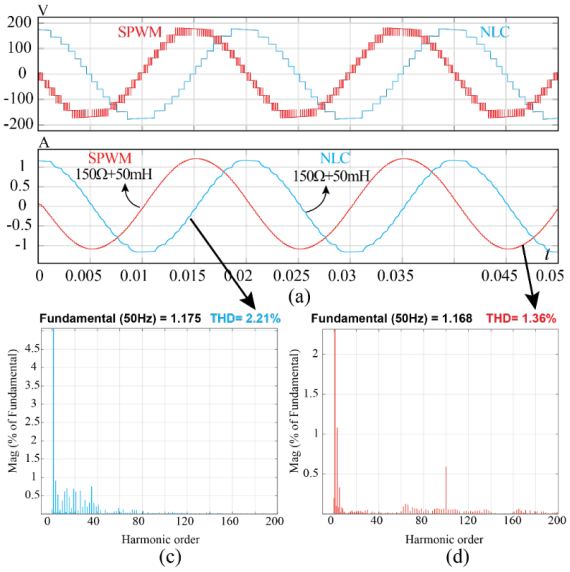

Fig. 3. Performance analysis of the proposed SC-MLI topology under SPWM and NLC control: (a) voltage and current responses; (b) harmonic distortion (THD) evaluation of the output current

Figure 4 illustrates how the proposed 13-level SC-MLI was set up for testing, and Table 4 lists the main sections that were used. A Genesys 2 Kintex-7 FPGA development board sent the power switches their control signals. You could program this board and control the switching accurately. The prototype was tested with both solely resistive and resistive-inductive loads. The inverter's output voltage always had a steady multilayer structure, no matter what the modulation index (MI) or switching frequency was. The results of the simulation and the real-world tests were remarkably similar, which shown that the design was correct and the suggested topology was very reliable.

Using an FPGA, a control platform makes control signals for the Near-Level Control (NLC) method at 50 Hz with a full modulation index. The initial test of the prototype was done with a load of $(150\,\Omega)$. Figure 5(a) illustrates the waveforms for the voltage and current that went with it. Inductors of $50mH$ and $200mH$ were connected in series with the resistive load to see how well the inverter worked with inductive loading. Figures 5(b) and 5(c) exhibit the output characteristics that show how the waveform's quality varies when the load inductance goes up. This demonstrates that the system maintains stable performance even when the load changes.

The influence of modulation index (MI) variation on the inverter's performance is shown in Figure 6. The 13-level SC-MLI was operated sequentially at MI values of 0.3, 0.6, and 1.0, followed by a return to 0.3. The robustness of the control strategy during these changes was demonstrated by the stability and uniformity of the output waveform. Similar to the frequency response analysis, detailed transient interval plots were included to more clearly illustrate the transient behavior.

Received: December 22, 2025. Reviewed: December 30, 2025. Accepted: December 30, 2025.

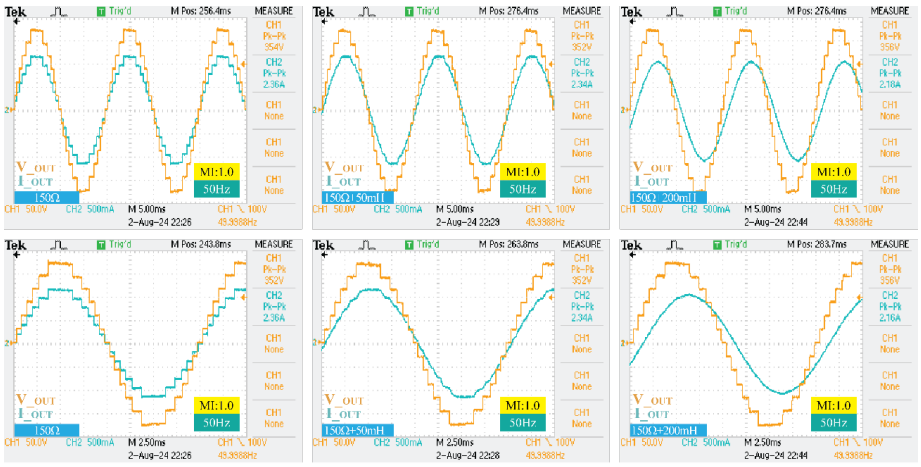

Fig. 4. Experimental evaluation under resistive and resistive–inductive loading: (a) 150 Ω resistive load, (b) (150 Ω + 50 mH) load, (c) (150 Ω + 200 mH) load

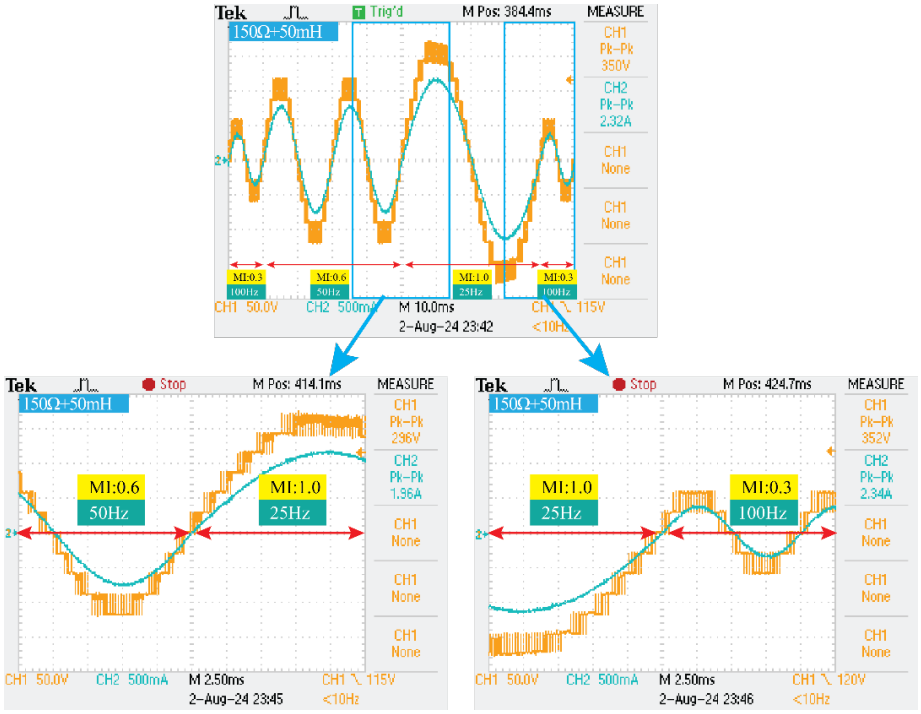

Fig. 5. Output voltage and current response of the proposed 13-level SC-MLI under modulation index and frequency variations

Received: December 22, 2025. Reviewed: December 30, 2025. Accepted: December 30, 2025.

V. Conclusion and Future Work

In this study, an innovative single-source switched-capacitor multilevel inverter (SC-MLI) architecture is proposed, which can provide 13 discrete voltage levels with a total of three gains. A comparative evaluation is carried out with the state-of-the-art solutions of the last three years, taking into account the main design parameters, including the number of semiconductor switches, the number of coupling capacitors and diodes, the total direct current voltage (TSV), the peak inverse voltage (PIV), and the overall cost efficiency. The results show that the proposed design requires fewer active and passive components compared to common single-source designs, which simplifies implementation, reduces hardware costs, and increases system reliability. Another key advantage is the self-balancing of capacitor voltages, which is achieved without the use of auxiliary sensors or additional control loops. Performance testing was carried out in sinusoidal pulse width modulation (SPWM) and near-level control (NLC) modes. Theoretical analysis, simulation results, and experimental studies consistently confirm the effectiveness of this topology. The results of comprehensive thermal simulations conducted in the PLECS environment showed that the system achieved an efficiency of up to 97.2% in the power range of 100–1000 W. However, during experiments performed in laboratory conditions, it was found that the practical efficiency value was at the level of 95.3%. In addition to meeting the harmonic distortion requirements, the proposed SC-MLI structure provides high energy efficiency despite the small number of elements. This unique combination allows us to consider this topology as a reliable and practical solution for next-generation multi-level inverters.

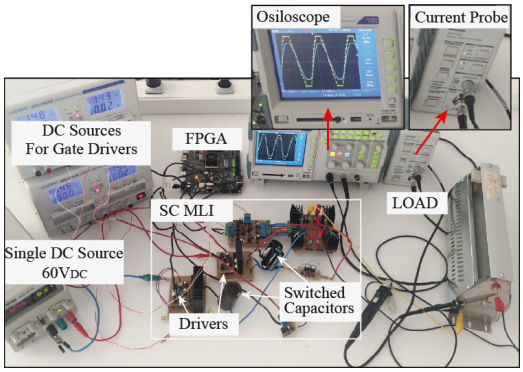

Fig. 6. Laboratory prototype and test bench configuration for the 13-level SC-MLI.

TABLE II
System Parameters and Components

PARAMETERS	
Input Voltage, V_{dc}	60 V
Output Voltage	180 V (peak)
Frequency	50 Hz
Max. Output Power	1000 W
COMPONENTS	
Capacitors	
C1	PG6DI (2200 μF, 600 V, ESR = 80 mΩ)
C2–C3	PG6DI (1200 μF, 600 V, ESR = 80 mΩ)
Power Devices	
IGBT	IGW60N60H3 (V_{CE} = 600 V, I_C = 60 A)
Fast-Recovery Diode	DSEI 60-06 (I_{FAV} = 60 A, V_{RRM} = 600 V, t_{rr} = 35 ns)
Controller	FPGA Development Board (Genesys 2 – Kintex-7)
Output Loads	Resistive (150 Ω), Inductive (50 mH + 200 mH)

Received: December 22, 2025. Reviewed: December 30, 2025. Accepted: December 30, 2025.

REFERENCES

[1] K. N. Taissariyeva and N. T. Issembergenov, "The Research of Multilevel Transistor Inverter for Converting Energy of Solar Panels," *Proceedings*, vol. 9662, pp. 197–203, 2015. DOI: 10.1117/12.2205605.

[2] M. Memis and M. Karakilic, "7-Level Soft Charging Switched Capacitor Multilevel Inverter," *IEEE Access*, 2025. DOI: 10.1109/ACCESS.2025.3560576.

[3] K. Jena, K. K. Gupta, D. Kumar, and S. RanjanKabat, "Single-Stage Single-Phase 5-Level Switched-Capacitor Multilevel Inverter," *Iranian Journal of Science and Technology: Transactions of Electrical Engineering*, vol. 48, pp. 265–276, 2024. DOI: 10.1007/s40998-023-00660-3.

[4] V. S. K. Prasadarao, S. Peddapati, and B. Kumar, "A Voltage-Boosting Seven-Level Switched Capacitor Multilevel Inverter With Reduced Device Count," *IEEE Journal of Emerging and Selected Topics in Power Electronics*, vol. 12, pp. 743–753, 2024. DOI: 10.1109/JESTPE.2023.3342123.

[5] J. Yao, X. Zheng, Z. Luo, Z. Zhang, and A. Ioinovici, "A Switched Capacitor Modified Fibonacci Cell Used for a DC-AC Circuit Supplied by Solar Energy," *IEEE Transactions on Circuits and Systems I: Regular Papers*, vol. 71, pp. 1933–1946, 2024. DOI: 10.1109/TCSI.2023.3349184.

[6] Z. Zhang, J. Yao, and A. Ioinovici, "Switched-Capacitor Multilevel Inverter With Input Source-Load Common Ground for Applications Supplied by Green Energy," *IEEE Transactions on Circuits and Systems II: Express Briefs*, vol. 71, pp. 186–190, 2024. DOI: 10.1109/TCSII.2023.3297321.

[7] M. Karakılıç, "A Novel Enhanced Switched Capacitor (ESC) Unit and ESC Based 9L MLI Topology," *Journal of Electrical Engineering & Technology*, 2025. DOI: 10.1007/s42835-025-02202-9.

[8] K. Taissariyeva and U. Seidaliyeva, "Design of Circuits of Multilevel Inverter on IGBT Transistors with Pulse-Amplitude Control," Proc. SPIE 10445, 2017. DOI: 10.1117/12.2280466.

[9] V. Anand and V. Singh, "A 13-Level Switched-Capacitor Multilevel Inverter With Single DC Source," *IEEE Journal of Emerging and Selected Topics in Power Electronics*, vol. 10, pp. 1575–1586, 2022. DOI: 10.1109/JESTPE.2021.3077604.

[10] S. Islam, M. D. Siddique, A. Iqbal, and S. Mekhilef, "A 9- and 13-Level Switched-Capacitor-Based Multilevel Inverter With Enhanced Self-Balanced Capacitor Voltage Capability," *IEEE Journal of Emerging and Selected Topics in Power Electronics*, vol. 10, 2022. DOI: 10.1109/JESTPE.2022.3179439.

[11] M. Karakılıç, J. Zeynalov, and H. Hatas, "Low-Cost Single-Source 17 Level Multilevel Inverter with Reduced Switch Count," *Engineering Research Express*, 2025. DOI: 10.1088/2631-8695/ADAAC1.

[12] T. Roy and P. K. Sadhu, "A Step-Up Multilevel Inverter Topology Using Novel Switched Capacitor Converters with Reduced Components," *IEEE Transactions on Industrial Electronics*, vol. 68, pp. 236–247, 2021. DOI: 10.1109/TIE.2020.2965458.

Received: December 22, 2025. Reviewed: December 30, 2025. Accepted: December 30, 2025.

SECTION III
Mathematics with Applied Aspects

This section includes applied mathematics research with a focus on modeling, optimization, and analysis of computational and engineering systems.

Article

Well-Posedness for a Degenerate Hyperbolic Equation with Weighted Initial Data

Nurbek Kakharman [1,2] and Aigul Zhumabayeva [1]

[1]Department of Mathematics and Natural Sciences, SDU University, Almaty, Kazakhstan
[2]Institute of Mathematics and Mathematical Modeling, Almaty, Kazakhstan

DOI: 10.47344/bgz8em14

Abstract

The focus of this study is an initial-boundary value problem associated with the degenerate hyperbolic equation $t\partial_{tt}u + \frac{1}{2}\partial_t u - \Delta u = g$ in a bounded domain. Due to the singularity at $t = 0$, standard initial conditions lead to an ill-posed problem. To achieve solvability of the problem, we introduce a "modified" Cauchy problem using weighted initial conditions for this degeneracy. The main result of the study is the proof of the well-posedness of this problem within the framework of classical Sobolev spaces, as well as the obtaining of a priori estimates of the solution. Furthermore, the general boundary conditions for the one-dimensional equation were derived by using the restriction and extension theory.

Keywords: degenerate hyperbolic equation, weighted initial condition, well-posed problem, spectral decomposition, weighted Sobolev space

I. Introduction

Degenerate partial differential equations are a significant and challenging area of mathematical physics [1]. Among them, degenerate hyperbolic equations, characterized by change of type or loss of strict hyperbolicity in certain domains or at certain moments in time, are of particular interest [2], [3]. Such equations are often found in mathematical models of various physical processes, especially in fluid and gas dynamics, and they arise naturally in classical elasticity and differential geometry.

The theory of strictly hyperbolic equations provides a clear and well-developed framework for the well-posedness of the Cauchy problem. However, the study of degenerate hyperbolic equations is associated with significant difficulties, see [4]–[7]. This complexity arises when a hyperbolic equation degenerates when the coefficients associated with lower-order terms within the hyperbolic equation become singular (see [8], [9]).

In general, obtaining well-posed solutions to the Cauchy problem for degenerate cases requires either imposing conditions on the coefficients or considering a "modified" initial condition. As noted in classical works [10], [11], the standard Cauchy problem for such equations may not be well-posed without appropriate modifications. Therefore, a natural approach is to study a weighted

Email: nurbek.kakharman@sdu.edu.kz, n.kakharman@math.kz ORCID: 0000-0002-1361-5552
Email: 241101003@sdu.edu.kz ORCID: 0009-0000-3015-2206

Received: December 19, 2025. Reviewed: December 25, 2025. Accepted: December 26, 2025.

Cauchy problem, in which the initial data are specified in a weighted form. This weighted formulation is essential to compensate for the singularity of the operator at $t = 0$ and to ensure that the solution remains bounded. For more details, see [12], [13] and the references therein.

In this work, we investigate a modified Cauchy problem for a degenerate hyperbolic equation considered in the cylindrical domain $D = (0, T) \times \Omega$, where $\Omega \subset R^n$ and $T > 0$. In addition, we provide a characterization of all possible regular boundary value problems associated with the corresponding singular ordinary differential equation by applying the restriction and extension theory, specifically relying on Otelbaev's abstract theorem.

II. Preliminaries

A. Inhomogeneous linear ODE with singular coefficient

Let us consider the following ODE

$$ly := ty''(t) + \frac{1}{2}y'(t) + \lambda y(t) = f(t), \quad t \in (0, T), \tag{1}$$

where $\lambda > 0$ is a fixed constant and f(t) is a given function.

First, we begin with the corresponding homogeneous equation

$$ty''(t) + \frac{1}{2}y'(t) + \lambda y(t) = 0. \tag{2}$$

It is well known that a fundamental system of solutions to this equation is given by the functions

$$y_1(t) = \cos 2\sqrt{\lambda t}, \quad y_2(t) = \sin 2\sqrt{\lambda t}.$$

To construct the general solution of (1), we apply the method of variation of parameters. We seek a solution in the form

$$y(t) = C_1(t)y_1(t) + C_2(t)y_2(t), \tag{3}$$

where $C_1(t)$ and $C_2(t)$ are functions to be determined. By imposing the standard condition $C_1'(t)y_1 + C_2'(t)y_2 = 0$, we arrive at the following linear system for the unknown derivatives $C_1'(t)$ and $C_2'(t)$:

$$\begin{cases} C_1'(t)y_1(t) + C_2'(t)y_2(t) = 0, \\ C_1'(t)y_1'(t) + C_2'(t)y_2'(t) = \dfrac{f(t)}{t}. \end{cases} \tag{4}$$

Substituting the explicit forms expressions for y_1 and y_2 and their derivatives we obtain

$$\begin{cases} C_1'(t)\cos 2\sqrt{\lambda t} + C_2'(t)\sin 2\sqrt{\lambda t} = 0, \\ -C_1'(t)\frac{\sqrt{\lambda}}{\sqrt{t}}\sin 2\sqrt{\lambda t} + C_2'(t)\frac{\sqrt{\lambda}}{\sqrt{t}}\cos 2\sqrt{\lambda t} = \dfrac{f(t)}{t}. \end{cases} \tag{5}$$

We determine the derivatives $C_1'(t)$ and $C_2'(t)$ from the linear system (5) by using Cramer's rule. We start by calculating the Wronskian determinant of the fundamental system

$$\begin{aligned} W &= \det \begin{pmatrix} \cos 2\sqrt{\lambda t} & \sin 2\sqrt{\lambda t} \\ -\sqrt{\dfrac{\lambda}{t}}\sin 2\sqrt{\lambda t} & \sqrt{\dfrac{\lambda}{t}}\cos 2\sqrt{\lambda t} \end{pmatrix}, \\ W &= \sqrt{\frac{\lambda}{t}}\cos 2\sqrt{\lambda t}\cdot\cos 2\sqrt{\lambda t} - \left(-\sqrt{\frac{\lambda}{t}}\sin 2\sqrt{\lambda t}\right)\cdot\sin 2\sqrt{\lambda t} \\ &= \sqrt{\frac{\lambda}{t}}\left[\cos^2 2\sqrt{\lambda t} + \sin^2 2\sqrt{\lambda t}\right] = \sqrt{\frac{\lambda}{t}}. \end{aligned} \tag{6}$$

Next, we compute the auxiliary determinants $W_1(t)$ and $W_2(t)$

$$W_1 = \det \begin{pmatrix} 0 & \sin 2\sqrt{\lambda t} \\ \dfrac{f(t)}{t} & \sqrt{\dfrac{\lambda}{t}}\cos 2\sqrt{\lambda t} \end{pmatrix} = -\frac{f(t)}{t}\sin 2\sqrt{\lambda t}, \tag{7}$$

Received: December 19, 2025. Reviewed: December 25, 2025. Accepted: December 26, 2025.

$$W_2 = \det \begin{pmatrix} \cos 2\sqrt{\lambda t} & 0 \\ -\sqrt{\frac{\lambda}{t}} \sin 2\sqrt{\lambda t} & \frac{f(t)}{t} \end{pmatrix} = \frac{f(t)}{t} \cos 2\sqrt{\lambda t}. \tag{8}$$

Consequently, the derivatives of the parameters are

$$C_1'(t) = \frac{W_1}{W} = -\frac{\sin 2\sqrt{\lambda t}}{\sqrt{\lambda t}} f(t), \tag{9}$$

$$C_2'(t) = \frac{W_2}{W} = \frac{\cos 2\sqrt{\lambda t}}{\sqrt{\lambda t}} f(t). \tag{10}$$

Integrating these expressions over the interval $(0, t)$, we find the functions $C_1(t)$ and $C_2(t)$

$$C_1(t) = \int_0^t -\frac{\sin 2\sqrt{\lambda \xi}}{\sqrt{\lambda \xi}} f(\xi) d\xi + c_1, \tag{11}$$

$$C_2(t) = \int_0^t \frac{\cos 2\sqrt{\lambda \xi}}{\sqrt{\lambda \xi}} f(\xi) d\xi + c_2, \tag{12}$$

where c_1 and c_2 are integration constants.

Inserting the obtained functions $C_1(t)$ and $C_2(t)$ into the general solution yields

$$\begin{aligned} y(t) = &- \cos 2\sqrt{\lambda t} \int_0^t \frac{\sin 2\sqrt{\lambda \xi}}{\sqrt{\lambda \xi}} f(\xi) d\xi + \sin 2\sqrt{\lambda t} \int_0^t \frac{\cos 2\sqrt{\lambda \xi}}{\sqrt{\lambda \xi}} f(\xi) d\xi \\ &+ c_1 \cos 2\sqrt{\lambda t} + c_2 \sin 2\sqrt{\lambda t}. \end{aligned} \tag{13}$$

To simplify the expression for the general solution (13), we group the terms under a single integral,

$$\begin{aligned} y(t) = &\int_0^t \frac{f(\xi)}{\sqrt{\lambda \xi}} \left[-\cos 2\sqrt{\lambda t} \sin 2\sqrt{\lambda \xi} + \sin 2\sqrt{\lambda t} \cos 2\sqrt{\lambda \xi} \right] d\xi \\ &+ c_1 \cos 2\sqrt{\lambda t} + c_2 \sin 2\sqrt{\lambda t}. \end{aligned} \tag{14}$$

Applying the sine difference formula, the general solution admits the compact representation:

$$y(t) = \int_0^t \frac{f(\xi)}{\sqrt{\lambda \xi}} \sin 2\sqrt{\lambda}(\sqrt{t} - \sqrt{\xi}) d\xi + c_1 \cos 2\sqrt{\lambda t} + c_2 \sin 2\sqrt{\lambda t}. \tag{15}$$

We next introduce the Cauchy problem associated with the operator l. To determine modified initial conditions, we investigate the behavior of the solution (15) as $t \to 0$. First, we examine $y(0)$

$$y(0) = \lim_{t \to 0} y(t) = c_1 \cdot 1 + c_2 \cdot 0 = c_1.$$

Hence, the requirement $y(0) = 0$ forces

$$c_1 = 0.$$

Let us next compute the derivative $y'(t)$. Differentiating expression (15) and simplifying yields

$$y'(t) = \int_0^t \frac{f(\xi)}{\sqrt{\xi t}} \cos\Big(2\sqrt{\lambda}(\sqrt{t} - \sqrt{\xi})\Big) d\xi \; + \; c_2 \frac{\sqrt{\lambda}}{\sqrt{t}} \cos 2\sqrt{\lambda t}. \tag{16}$$

Because the term $c_2 \frac{\sqrt{\lambda}}{\sqrt{t}} \cos 2\sqrt{\lambda t}$ is unbounded as $t \to 0$, the derivative $y'(t)$ itself cannot be prescribed directly at $t = 0$. Instead, we analyze the limit of the weighted expression $\sqrt{t} \frac{d}{dt} y(t)$:

$$\lim_{t \to 0} \sqrt{t} \frac{d}{dt} y(t) = 0 + c_2 \sqrt{\lambda}.$$

For this weighted limit to remain finite, we must take $c_2 = 0$. This choice provides the second initial condition

$$\lim_{t \to 0} \sqrt{t} \frac{d}{dt} y(t) = 0.$$

Received: December 19, 2025. Reviewed: December 25, 2025. Accepted: December 26, 2025.

As a result, the conditions defining a well-posed problem for the differential operator (1) are given below

$$y(0) = 0, \quad \lim_{t\to 0} \sqrt{t}\, \frac{d}{dt} y(t) = 0.$$

We can now state the full Cauchy problem as

$$\begin{cases} ty''(t) + \frac{1}{2}y'(t) + \lambda y(t) = f(t), \\ y(0) = 0, \ \lim_{t\to 0^+} \sqrt{t}\, \frac{d}{dt} y(t) = 0. \end{cases} \tag{17}$$

And finally, the solution to the Cauchy problem is as follows

$$y(t) = \int_0^t \frac{f(\xi)}{\sqrt{\lambda \xi}} \sin 2\sqrt{\lambda}(\sqrt{t} - \sqrt{\xi}) d\xi. \tag{18}$$

B. Eigenvalue problem for the Laplace operator

In this section, we provide the definition of the eigenvalue problem for the Laplace operator with homogeneous Dirichlet boundary conditions, followed by the associated lemma and theorem:

$$\begin{cases} -\Delta \varphi(x) = \lambda \varphi(x), & x \in \Omega, \\ \varphi(x) = 0, & x \in \partial\Omega. \end{cases} \tag{19}$$

The eigenfunctions $\{\varphi_k(x)\}_{k=1}^{\infty}$ of the self-adjoint problem (19) form a complete orthonormal basis for $L^2(\Omega)$, with eigenvalues satisfying $0 < \lambda_1 \le \lambda_2 \le \cdots \to \infty$ (see, e.g., [14]).

Lemma II.1 (Orthogonality and simplicity [14])**.** *The eigenfunctions $\{\varphi_k(x)\}_{k=1}^{\infty}$ corresponding to the eigenvalues λ_k form an orthonormal system in $L^2(\Omega)$, i.e.,*

$$(\varphi_k, \varphi_m)_{L^2(\Omega)} = \int_\Omega \varphi_k(x)\varphi_m(x)\, dx = \delta_{km},$$

where δ_{km} is the Kronecker delta.

Theorem II.2 (Spectral decomposition and completeness [14])**.** *The system of eigenfunctions $\{\varphi_k(x)\}_{k=1}^{\infty}$ is complete in $L^2(\Omega)$.*

III. Main results

A. Formulation of the Modified Cauchy Problem in a Bounded Domain

Let $\Omega \subset R^n$ be a bounded domain with a sufficiently smooth boundary, specifically $\partial\Omega \in C^2$. We introduce the cylindrical domain defined by $D = (0, T) \times \Omega$. Given a source function $g \in L^2(D)$, we seek a function u that satisfies

$$Lu = tu_{tt} + \frac{1}{2}u_t - \Delta u = g(t, x), \quad (t, x) \in D. \tag{20}$$

The equation is supplemented by the following initial conditions

$$u(0, x) = 0, \qquad \lim_{t\to 0} \sqrt{t} u_t(t, x) = 0, \quad x \in \Omega, \tag{21}$$

and the homogeneous Dirichlet boundary condition

$$u(t, x)\big|_{x\in\partial\Omega} = 0, \quad t \in [0, T]. \tag{22}$$

To solve problem (20)–(22) we employ the method of spectral decomposition. Consider the complete orthonormal system $\{\varphi_k(x)\}_{k=1}^{\infty}$ in $L_2(\Omega)$, consisting of eigenfunctions of the spectral problem (19), and let $\{\lambda_k\}_{k=1}^{\infty}$ be the corresponding eigenvalues.

According to Theorem II.2, both the solution and the source function can be expanded into Fourier series

$$u(t, x) = \sum_{k=1}^{\infty} \varphi_k(x) y_k(t), \qquad g(t, x) = \sum_{k=1}^{\infty} \varphi_k(x) g_k(t), \tag{23}$$

Received: December 19, 2025. Reviewed: December 25, 2025. Accepted: December 26, 2025.

where the expansion coefficients are given by

$$y_k(t) = \int_\Omega \varphi_k(x)u(t,x)\,dx, \qquad g_k(t) = \int_\Omega \varphi_k(x)g(t,x)\,dx. \tag{24}$$

From the initial conditions (21), it follows that for the coefficients $y_k(t)$ satisfy

$$y_k(0) = 0, \qquad \lim_{t\to 0}\sqrt{t}y_k'(t) = 0.$$

Substitution of the series representation (23) into equation (20) reduces the partial differential equation to a one-dimensional singular Cauchy problem for the coefficient y_k

$$l_k y_k := ty_k''(t) + \frac{1}{2}y_k'(t) + \lambda_k y_k(t) = f_k(t), \tag{25}$$

$$y_k(0) = 0, \qquad \lim_{t\to 0}\sqrt{t}y_k'(t) = 0. \tag{26}$$

As established in the previous sections, the homogeneous equation $l_k y_k = 0$ possesses solutions spanned by trigonometric functions giving the general homogeneous solution as

$$y_{k,h}(t) = C_1\cos(2\sqrt{\lambda_k t}) + C_2\sin(2\sqrt{\lambda_k t}). \tag{27}$$

Employing the variation of parameters method and applying the initial conditions (26) provides the unique solution to the singular Cauchy problem (25)–(26):

$$y_k(t) = \int_0^t \frac{f_k(\xi)}{\sqrt{\lambda_k \xi}}\sin\left[2\sqrt{\lambda_k}(\sqrt{t}-\sqrt{\xi})\right]d\xi. \tag{28}$$

Finally, substituting expression (28) back into (23) leads to the following representation of the solution to (20)–(22):

$$u(t,x) = \sum_{k=1}^{\infty}\varphi_k(x)\left(\int_0^t \frac{f_k(\xi)}{\sqrt{\lambda_k\xi}}\sin\left[2\sqrt{\lambda_k}(\sqrt{t}-\sqrt{\xi})\right]d\xi\right). \tag{29}$$

B. Sobolev Regularity for the Singular ODE

We introduce the weighted Sobolev space $W^2_{2,t}(0,T) = \{y : y \in L^2(0,T) \text{ and } ty'' \in W^1_2(0,T)\}$ with the norm

$$\|y\|_{W^2_{2,t}(0,T)} := \left\|t\frac{d^2}{dt^2}y\right\|_{L^2(0,T)} + \left\|\frac{d}{dt}y\right\|_{L^2(0,T)} + \|y\|_{L^2(0,T)}. \tag{30}$$

Lemma III.1. *Let $f_k \in L^2(0,T)$. Then the solution $y_k \in W^2_{2,t}(0,T)$ of the one-dimensional singular equation* (25)–(26) *satisfies the estimate*

$$\|y_k\|_{W^2_{2,t}(0,T)} \le c\|f_k\|_{L^2(0,T)},$$

where c is a constant.

Proof. Let $v = \sqrt{t}$ and define $w(v) = y(v^2)$. Then $y(t) = w(\sqrt{t})$, and computing derivatives yields

$$w''(v) + 4\lambda w(v) = 4f(v^2).$$

The solution (28) has the form

$$w(y) = \frac{2}{\sqrt{\lambda}}\int_0^v \sin\big(2\sqrt{\lambda}(v-s)\big)g(s)ds,$$

with derivative

$$w'(v) = 4\int_0^v \cos\big(2\sqrt{\lambda}(v-s)\big)g(s)ds.$$

Define $g(v) = f(v^2)$. Since $f \in L^2(0,T)$, we have

$$\int_0^{\sqrt{T}} v|g(v)|^2 dy < \infty.$$

Received: December 19, 2025. Reviewed: December 25, 2025. Accepted: December 26, 2025.

We show $y_k \in W_2^1(0,T)$ by proving

$$\int_0^T |y_k(t)|^2 dt < \infty \quad \text{and} \quad \int_0^T |y_k'(t)|^2 dt < \infty.$$

Using the substitution $t = v^2$, these become

$$\int_0^{\sqrt{T}} v|w(v)|^2 dv < \infty \quad \text{and} \quad \int_0^{\sqrt{T}} \frac{|w'(v)|^2}{v} dv < \infty.$$

From the solution representation, we have the bounds

$$|w(v)| \le \frac{2}{\sqrt{\lambda}} \int_0^v |g(s)| ds, \quad |w'(v)| \le 4 \int_0^v |g(s)| ds.$$

Using the bound on w, Cauchy–Schwarz, and Fubini's theorem, we obtain

$$\int_0^{\sqrt{T}} v|w(v)|^2 dv \le \frac{16}{5\lambda_k} T^{5/4} \int_0^{\sqrt{T}} s|g(s)|^2 ds < \infty.$$

Similarly, with the bound for w', we obtain

$$\int_0^{\sqrt{T}} \frac{|w'(v)|^2}{v} dv \le 64 T^{1/4} \int_0^{\sqrt{T}} s|g(s)|^2 ds < \infty.$$

Using the transformation $t = v^2$, we obtain the following L^2 bounds

$$\|y_k\|_{L^2(0,T)} \le \frac{4}{\sqrt{5\lambda_k}} T^{5/8} \|f_k\|_{L^2(0,T)}, \tag{31}$$

and

$$\|y_k'\|_{L^2(0,T)} \le 4T^{1/8} \|f_k\|_{L^2(0,T)}. \tag{32}$$

Which concludes

$$\int_0^T |y_k(t)|^2 dt < \infty \quad \text{and} \quad \int_0^T |y_k'(t)|^2 dt < \infty.$$

Equation (25) can be rearranged to express the second derivative term:

$$t y_k''(t) = f_k(t) - \frac{1}{2} y_k'(t) - \lambda_k y_k(t),$$

From this, it can be concluded that

$$\begin{aligned} \|t y_k''\|_{L^2(0,T)} \le & \|f_k\|_{L^2(0,T)} + \|\frac{1}{2} y_k'\|_{L^2(0,T)} + \|\lambda_k y_k\|_{L^2(0,T)} \\ \le & c\|f_k\|_{L^2(0,T)}. \end{aligned} \tag{33}$$

C. Solution estimates for general case

We define the $(-\Delta_x)^{\frac{1}{2}}$ acting on a function $g \in L^2(D)$ by the following rule

$$(-\Delta_x)^{\frac{1}{2}} g = \sum_{k=1}^{\infty} g_k(t) \sqrt{\lambda_k} \varphi_k(x), \tag{34}$$

with the norm $\|(-\Delta_x)^{\frac{1}{2}} g\|^2_{L^2(D)} = \sum\limits_{k=1}^{\infty} \lambda_k |g_k(t)|^2$.

Let $W^{2,2}_{2,t}(D)$ be the weighted Sobolev space with the norm

$$\|u\|_{W^{2,2}_{2,t}} := \left\| t \frac{\partial^2 u}{\partial t^2} \right\|_{L^2(D)} + \left\| \frac{\partial u}{\partial t} \right\|_{L^2(D)} + \|\Delta u\|_{L^2(D)} + \|u\|_{L^2(D)}. \tag{35}$$

Received: December 19, 2025. Reviewed: December 25, 2025. Accepted: December 26, 2025.

Theorem III.2. *Assume that $g \in L^2(D)$ and that the condition*
$\sum_{|m|=1}^{\infty} \lambda_m |g_m(\xi)|^2 < \infty$ *holds. Then there exists a unique solution $u \in W_{2,t}^{2,2}(D)$ of the problem* (20)- (22) *that satisfies the following inequality*

$$\left\| t\frac{\partial^2 u}{\partial t^2} \right\|_{L^2(D)} + \left\| \frac{\partial u}{\partial t} \right\|_{L^2(D)} + \|\Delta_x u\|_{L^2(D)} + \|u\|_{L^2(D)} \le c\|g\|_{L^2(D)} + c_0 \left\| (-\Delta_x)^{\frac{1}{2}} g \right\|_{L^2(D)},$$

with constants c and c_0 depending only on T.

Proof. By Parseval's identity, we have

$$\|u\|_{L^2(D)}^2 = \sum_{k=1}^{\infty} |y_k(t)|^2 \, dt \le c_1 \int_0^T \sum_{k=1}^{\infty} \left(\frac{1}{\lambda_k} |g_k(t)|^2 \right) dt.$$

By (31) and $\sum_{k=1}^{\infty} \frac{1}{\lambda_k} \|g_k(t)\|^2 \le \frac{1}{\lambda_1} \sum_{k=1}^{\infty} \|g_k(t)\|^2$, we obtain

$$\|u\|_{L^2(D)}^2 \le c_1 \sum_{k=1}^{\infty} \|g_k\|_{L^2(0,T)}^2 = c_1 \|g\|_{L^2(D)}^2.$$

Similarly, by (32) we get

$$\left\| \frac{\partial u}{\partial t} \right\|_{L^2(D)}^2 \le c_2 \|g\|_{L^2(D)}^2.$$

Similar considerations apply to $\Delta_x u$, from (31), we have

$$\|\Delta_x u\|_{L^2(D)} = \sum_{k=1}^{\infty} |\lambda_k y_k(t)|^2 \le c \|(-\Delta_x)^{\frac{1}{2}} g\|_{L^2(D)}^2.$$

Finally, rewriting equation (20) as

$$t\frac{\partial^2 u}{\partial t^2} = g(t,x) - \frac{1}{2}\frac{\partial u}{\partial t} + \Delta u.$$

Now it is easily seen that

$$\left\| t\frac{\partial^2}{\partial t^2} u \right\|_{L^2(D)} \le c\|g\|_{L^2(D)} + c_0 \left\| (-\Delta_x)^{\frac{1}{2}} g \right\|_{L^2(D)}. \tag{36}$$

This proves the theorem.

IV. Regular boundary value problem for the second-order equation

The aim of this section is to obtain general boundary conditions for equation (1) in the one-dimensional case. Our approach relies on extension and restriction theory for differential operators, and in particular on the abstract theorem of Otelbaev [15].

Defining the correct boundary conditions requires deriving the conjugate problem for the operator l (1). The calculation of the scalar product yields

$$\langle ty'' + \frac{1}{2}y' + \lambda y, w \rangle = \langle y, tw'' + \frac{3}{2}w' + \lambda w \rangle.$$

Thus, the conjugate operator is

$$l^* w = t\, w'' + \frac{3}{2}\, w' + \lambda w.$$

Consequently, the Cauchy problem admits the following conjugate formulation

$$\begin{cases} tw''(t) + \frac{3}{2}w'(t) + \lambda w(t) = \phi(t), \\ w(1) = 0, \;\; w'(1) = 0. \end{cases} \tag{37}$$

The homogeneous problem

$$tw''(t) + \frac{3}{2}w'(t) + \lambda w(t) = 0,$$

Received: December 19, 2025. Reviewed: December 25, 2025. Accepted: December 26, 2025.

has a general solution of the following form

$$w(t) = -q_1\sqrt{\frac{\lambda}{t}}\sin 2\sqrt{\lambda t} + q_2\sqrt{\frac{\lambda}{t}}\cos 2\sqrt{\lambda t}. \tag{38}$$

where q_1, q_2 are arbitrary constants.

Now let us return to our general solution (15), where constants c_1 and c_2 that depend continuously and linearly on f; that is,

$$c_1 = c_1(f), c_2 = c_2(f).$$

By the Riesz representation theorem, these functionals can be expressed as

$$c_1 = \int_0^1 \sigma_1(t)f(t)dt,\ c_2 = \int_0^1 \sigma_2(t)f(t)dt,$$

where σ_1 and σ_2 belong to the kernel of the operator (37) (see [15]). We choose them in the form

$$\sigma_1(t) = -q_1\sqrt{\frac{\lambda}{t}}\ \sin 2\sqrt{\lambda t}, \quad \sigma_2(t) = q_2\sqrt{\frac{\lambda}{t}}\ \cos 2\sqrt{\lambda t}.$$

Consequently, we obtain

$$c_1 = -q_1\int_0^1 \sqrt{\frac{\lambda}{t}}\sin 2\sqrt{\lambda t}f(t)dt,\ c_2 = q_2\int_0^1 \sqrt{\frac{\lambda}{t}}\cos 2\sqrt{\lambda t}f(t)dt.$$

Substituting these integral expressions into (15), we derive the following expression for $y(t)$:

$$\begin{aligned} y(t) = &\int_0^t \frac{f(\xi)}{\sqrt{\lambda\xi}}\sin 2\sqrt{\lambda}(\sqrt{t}-\sqrt{\xi})d\xi - \\ &- q_1\cos 2\sqrt{\lambda t}\int_0^1 \sqrt{\frac{\lambda}{t}}\sin 2\sqrt{\lambda t}f(t)dt + q_2\sin 2\sqrt{\lambda t}\int_0^1 \sqrt{\frac{\lambda}{t}}\cos 2\sqrt{\lambda t}f(t)dt. \end{aligned} \tag{39}$$

Evaluating the integrals in (39) using integration by parts and rearranging the terms, we arrive at the corresponding boundary value problem for equation (1):

$$\begin{cases} -y(0) + q_1\left(-y'(1)\sqrt{\lambda}\sin(2\sqrt{\lambda}) + y(1)\cos(2\sqrt{\lambda}) - \lambda y(0)\right) = 0, \\ \lim\limits_{t\to 0+}\dfrac{y'(t)\sqrt{t}}{\sqrt{\lambda}} + q_2\left(y'(1)\sqrt{\lambda}\cos(2\sqrt{\lambda}) + \lambda y(1)\sin(2\sqrt{\lambda})\right) = 0. \end{cases} \tag{40}$$

It is not difficult to observe that in the special case when the free constants q_1, q_2 are zero, we obtain the Cauchy problem. Writing this boundary condition in matrix form

$$\begin{pmatrix} -1-aq_1 & aq_1\cos 2\sqrt{a} & 0 & -\sqrt{a}q_1\sin 2\sqrt{a} \\ 0 & a\sqrt{a}q_2\sin 2\sqrt{a} & -1 & aq_2\cos 2\sqrt{a} \end{pmatrix} \begin{pmatrix} y(0) \\ y(1) \\ \lim_{t\to 0+}\sqrt{t}y'(t) \\ y'(1) \end{pmatrix} = 0. \tag{41}$$

The obtained results allow us to state the theorem

Theorem IV.1. *The differential equation* (1) *has a unique solution satisfying the boundary condition* (41) *for all* $f \in L^2(0,1)$ *and every* $q_1, q_2 \in R$.

V. Conclusion

In this work, we investigated the initial-boundary value problem for a degenerate hyperbolic equation with a singularity at $t = 0$ by introducing a modified Cauchy problem with weighted initial conditions. We proved the well-posedness of this problem in the weighted Sobolev space $W_{2,t}^{2,2}(D)$, derived the necessary a priori estimates for the solution, and using the theory of operator extension, characterized the general regular boundary conditions for the corresponding one-dimensional singular ordinary differential equation.

Received: December 19, 2025. Reviewed: December 25, 2025. Accepted: December 26, 2025.

ACKNOWLEDGEMENTS

This research was funded by the Science Committee of the Ministry of Science and Higher Education of the Republic of Kazakhstan (Grant No. AP22785364).

REFERENCES

[1] Bitsadze, A. V., *Some Classes of Partial Differential Equations*, Nauka, Moscow, 1981 (in Russian).

[2] Krasnov, M. L., Mixed boundary value problems for degenerate linear hyperbolic differential equations of second order, *Matematicheskii Sbornik*, 91:1 (1959), 29–77 (in Russian).

[3] Bitsadze, A. V., Nakhushev, A. M., On the theory of degenerate hyperbolic equations in multidimensional domains, *Doklady Akademii Nauk SSSR*, 204 (1972), 1289–1291

[4] O. A. Olêinik, *On the Cauchy problem for weakly hyperbolic equations*, Comm. Pure Appl. Math., 23 (1970), 569-586.

[5] V.N. Vragov, *Boundary value problems for nonclassical equations of mathematical physics*, Novosibirsk, NGU, 1983. (in Russian)

[6] S. A. Tersenov, *Introduction to the Theory of Equations that are Degenerate on the Boundary*, Novosibirsk Univ. Press, Novosibirsk, 1973 (in Russian).

[7] R. W. Carroll and R. E. Showalter, *Singular and Degenerate Cauchy Problems*, Academic Press, New York, 1976.

[8] Smirnov, M. M., *Degenerate hyperbolic equations*, Minsk, 1977 (in Russian).

[9] Colombini, F., Spagnolo, S., An example of a weakly hyperbolic Cauchy problem not well posed in C^∞, *Acta Math.*, 148 (1982), 243–253.

[10] Oleinik, O. A., On the Cauchy problem for weakly hyperbolic equations, *Communications on Pure and Applied Mathematics*, 23 (1970), 569–586.

[11] F. Colombini, E. Jannelli, and S. Spagnolo, *Well-posedness in the Gevrey classes of the Cauchy problem for a non-strictly hyperbolic equation with coefficients depending on time*, Annali della Scuola Normale Superiore di Pisa-Classe di Scienze, 10 (2) (1983), 291-312.

[12] Kakharman, N., Kal'menov, T., Mixed Cauchy problem with lateral boundary condition for noncharacteristic degenerate hyperbolic equations, *Boundary Value Problems*, 2022:1 (2022), 35.

[13] Kakharman, N., Kalmenov, T. Sh., A Modified Cauchy Problem With Nonlocal Boundary Condition for a Degenerate Hyperbolic Equation, *Mathematical Methods in the Applied Sciences*, 48:8 (2025), 9313–9319.

[14] Henrot, A., *Extremum Problems for Eigenvalues of Elliptic Operators*, Springer, 2006.

[15] B. K. Kokebaev, M. Otelbaev, A. N. Shynybekov, *On the theory of contraction and extension of operators I*, Izv. Akad. Nauk Kazakh SSR, Ser. Fiz.-Mat., 5 (1982), 24–26.

Received: December 19, 2025. Reviewed: December 25, 2025. Accepted: December 26, 2025.

End of Volume 3, Issue 3

Journal of Emerging Technologies and Computing (JETC)

Published by SDU University • © 2025